

# Journal of Applied Math

<https://ojs.acad-pub.com/index.php/JAM>



ACADEMIC  
ACADEMIC PUBLISHING PTE LTD

2023 VOLUME 1 ISSUE 1  
ISSN: 2972-4805



ISSN 2972-4805



9 772972 480012

01 >

1



## Editorial Board

### Editor-in-Chief

**Ahmad Zeeshan**  
International Islamic University  
Pakistan

### Editorial Board Member

**Kottakkaran Sooppy Nisar**  
Prince Sattam Bin Abdulaziz University  
Saudi Arabia

**Stojan Novica Radenovic**  
University of Belgrade  
Serbia

**Nehad Ali Shah**  
Sejong University  
Korea, Republic of

**Sara Ibrahim Abdelsalam**  
The British University in Egypt  
Egypt

**Sivasankaran Sivanandam**  
King Abdulaziz University  
Saudi Arabia

**Satyaranjan Mishra**  
Siksha 'O' Anusandhan (Deemed to be  
University)  
India

**Madjid Eshaghi Gordji**  
Semnan University  
Iran, Islamic Republic of

**Samer Ezz-Eldien**  
New Valley University  
Egypt

**Waqas Nazeer**  
Government College University Lahore  
Pakistan

**Muhammad Abbas**  
University of Sargodha  
Pakistan

**Wenpeng Zhang**  
Northwest University  
China

**Muhammad Arshad**  
Abbottabad University of Science and  
Technology  
Pakistan

**Sadia Siddiq**  
Prince Sultan University  
Saudi Arabia

**Ramalingam Udhayakumar**  
Vellore Institute of Technology  
India

**Kifayat Ullah**  
Riphah International University  
Pakistan

**Bibhya Sharma**  
University of the South Pacific  
Fiji

**Vladimir Cheverda**  
Sobolev Institute of Mathematics  
Russian Federation

**Len Gelman**  
University of Huddersfield  
United Kingdom

**Anca Voichita Matic**  
Universität Regensburg  
Germany

**Muhammad Shoaib Anwar**  
University of Jhang  
Pakistan

**Qasim Ali Arain**

Mehran University of Engineering and  
Technology  
Pakistan

**Jeff Morgan**

University of Houston  
United States

**Afshin Babaei**

University of Mazandaran  
Iran, Islamic Republic of

**Yunhu Wang**

Shanghai Maritime University  
China

**William Fitzgibbon**

University of Houston  
United States

**Ehsan Hatefi**

Scuola Normale Superiore  
Italy

**Shaoxin Sun**

Chongqing University  
China

**Francisco Javier García Pacheco**

University of Cadiz  
Spain

**Hüseyin Kamacı**

Yozgat Bozok University  
Turkey

**Ercan Çelik**

Kyrgyz-Turkish Manas University  
Kyrgyzstan

**Timothy Sands**

Cornell University  
United States

**D.L. Suthar**

Wollo University  
Ethiopia

**Natalia Bebiano**

University of Coimbra  
Portugal

**Hasan Koten**

Istanbul Medeniyet University  
Turkey

**Zoubir Dahmani**

University of Mostaganem  
Algeria

**Teodor Bulboaca**

Babeş-Bolyai University of Cluj-Napoca  
Romania

**Minking Eie**

National Chung Cheng University  
Taiwan, Province of China

**Mikhail B. Sheftel**

Boğaziçi Üniversitesi  
Turkey

**S. Eswaramoorthi**

Dr. N.G.P. Arts and Science College  
India

**Abdullah Alsharif**

Taif University  
Saudi Arabia

**Vladimir Valentinovich Egorov**

Photochemistry Center of the Russian  
Academy of Sciences  
Russian Federation

**Roger Mboupda**

University of Dschang  
Cameroon

Volume 1 Issue 1 • 2023

# Journal of AppliedMath

**Editor-in-Chief**

**Ahmad Zeeshan**

*International Islamic University, Pakistan*



# Journal of AppliedMath

<https://ojs.acad-pub.com/index.php/JAM/index>

## Contents

- 1 Novel learning for control of nonlinear spacecraft dynamics**  
*Bo-Ruei Huang, Timothy Sands*
- 21 Statistical analysis of a Tagore song based on Raga Kafi**  
*Soubhik Chakraborty, Prerna Singh*
- 28 Machine learning in coal and gas outburst prediction**  
*Peng Ji, Shiliang Shi*
- 30 Towards a solution to the problem of safety management of structurally complex systems**  
*Alexander V. Bochkov*
- 45 Sustainable information into portfolio optimization models**  
*Gabriele Sbaiz*
- 48 Impact of Hindustani ragas in stress management: A statistical study**  
*Soubhik Chakraborty, Avinav Prasad, Apoorva Chakraborty, Prerna Singh*
- 55 Conservation laws, exact solutions and nonlinear dispersion: A lie symmetry approach**  
*Adnan Shamaoon, Zartab Ali, Qaisar Maqbool*

# Novel learning for control of nonlinear spacecraft dynamics

Bo-Ruei Huang<sup>1</sup>, Timothy Sands<sup>2\*</sup>

<sup>1</sup> Sibley School of Mechanical and Aerospace Engineering, Cornell University, Ithaca, New York 14853, USA.

<sup>2</sup> Department of Mechanical Engineering (SCPD), Stanford University, Stanford 94305, USA. E-mail: dr.timsands@alumni.stanford.edu

## ARTICLE INFO

Received: 10 February 2023

Accepted: 4 March 2023

Available online: 12 April 2023

<http://dx.doi.org/10.59400/jam.v1i1.42>

Copyright © 2023 Author(s).

*Journal of AppliedMath* is published by Academic Publishing Pte. Ltd. This article is licensed under the Creative Commons Attribution-NonCommercial 4.0 International License (CC BY-NC 4.0).  
<https://creativecommons.org/licenses/by-nc/4.0/>

**ABSTRACT:** With accurate dynamic system parameters (embodied in self-awareness statements), a controller can provide precise signals for tracking desired state trajectories. If dynamic system parameters are initially guessed inaccurately, a learning method may be used to find the accurate parameters. In the deterministic artificial intelligence method, self-awareness statements are formed as mathematical expressions of the governing physics. When the nonlinear, coupled expressions are precisely parameterized as the product of known matrix components and unknown vectrix (i.e., an intermediate between a dyadic and a matrix in regression form) tracking errors may be projected onto the known matrix to update the unknown vectrix in an optimal form (in a two-norm sense). In this work, a modified learning method is proposed and proved to have global convergence of both state error and parameter estimation error. The modified learning method is compared with those in the prequels using simulation experiments of three-dimensional rigid body dynamic rotation motion. The achieved state error convergence using the modified approach is two magnitudes better than using the methods in the prequels.

**KEYWORDS:** nonlinear systems; mechanics; spacecraft attitude control; deterministic artificial intelligence; regression; learning

## 1. Introduction

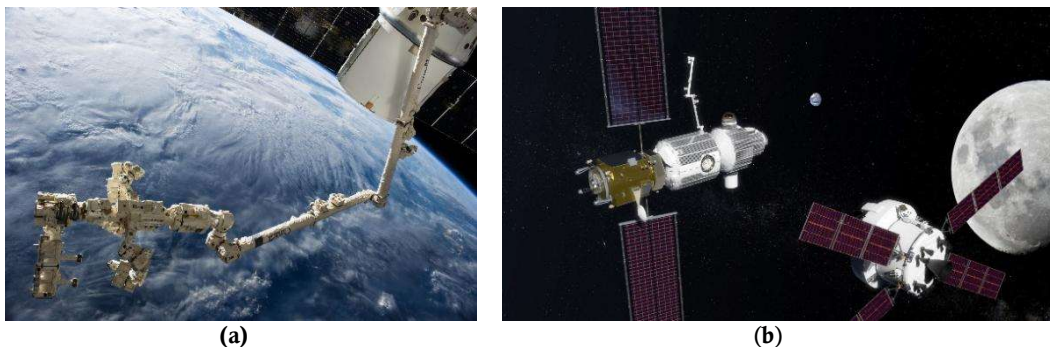


**Figure 1.** (a) The International Space Station's Canadarm2 and Dextre carry the RapidScat instrument assembly after removing it from the trunk of the SpaceX Dragon cargo ship (upper right), which is docked at the nadir port of the Harmony node. (b) NASA Gateway would support a growing space economy photos taken from [1] and [2] respectively in compliance with NASA's image use policy<sup>[3]</sup>.

Consider intricate robotic operations in low-earth orbit near the space station as displayed in **Figure 1**, where considerable human

intervention is available. Next, contemplate the requirements to autonomously do such operations in far distant cis-lunar orbits. The latter sys-

tem must be able to learn in real-time dynamic changes that occur when the space robot grasps and grapples targeted spacecraft. Dynamics and control issues associated with rendezvous in Cis-lunar space near rectilinear halo orbits were investigated in [4], where a fully-safe, automatic rendezvous strategy was developed between a passive vehicle and an active one orbiting around the Earth-Moon L2 Lagrangian point. Bando *et al.*<sup>[4]</sup> proposed a chattering attenuation sliding mode control utilizing the eigen structure of the linearized flow around a libration point of the Earth-Moon circular restricted three-body problem, and this novel article serves as a reminder of the prevalence of linearization when dealing with multiple, coupled nonlinear equations. In 2021, Colombia presented a guidance, navigation and control framework for 6 degrees of freedom (6DOF) coupled Cislunar rendezvous and docking, and the article highlighted the importance of dealing with full, coupled translational-rotational dynamics of multi-body (i.e., highly flexible) dynamics seeking guaranteed coupled-state estimation<sup>[5]</sup>. Immediately that same year<sup>[6]</sup>, new techniques for highly flexible multi-body space robotics were proposed as a competing narrative to the just-proposed “whiplash compensation” of flexible space robotics<sup>[7]</sup> establishing a thread of research offered by Cornell University. China now has two robotic arms attached to its space station<sup>[8]</sup>, where a large robotic arm can “crawl” along the outside of the spacecraft<sup>[9]</sup>.

An alternative thread of research is offered by Massachusetts Institute of Technology<sup>[10–16]</sup>. Noting that ubiquitous approaches rely on either simplifying assumptions in the dynamical model or on abundant computational resources, Lafarge *et al.*<sup>[10]</sup> proposed reinforcement learning for closed-loop control of onboard low-thrust guidance. Albee *et al.*<sup>[11]</sup> studied active interception of targets for autonomous repair and deorbiting must account for the tumbling motion of targets, which is oftentimes not known a priori. A model reference adaptive algorithmic approach was proposed to identify the state of the target’s tum-

ble. In a more typical manner, Mehta *et al.*<sup>[12]</sup> proposed a quasi-physical dynamic reduced-order model that used a linear approximation of the underlying dynamics and effect of the drivers where data assimilation and model calibration utilized estimation of the model coefficients that represent the model parameters. One sequel article about autonomous docking with rotating targets via reinforcement learning was offered by Oestreich *et al.*<sup>[13]</sup> proposing learning policies. Following the initial target search<sup>[14]</sup>, analytical closed expressions to compute the minimum distance between any two satellites (at the same altitude in circular orbits), Avendaño *et al.* proposed “flower constellations” to produce give an efficient method to compute the minimum angular distance between satellites. Reversing the method, Arnas *et al.*<sup>[15]</sup> proposed two-dimensional lattice flower constellations to design a low earth orbit slotting system to avoid collisions between compliant satellites (rather than intercept). Oestreich *et al.*<sup>[16]</sup> also highlighted dependence on on-orbit inspection (i.e., relative navigation and inertial properties estimation) to intercept tumbling debris objects or defunct satellites. In a late proposal following the M.I.T. approach, the master’s thesis by Roberts<sup>[17]</sup> continued to develop the stochastic artificial intelligence approach embodied in supervised learning. Ekal *et al.*<sup>[18]</sup> highlight key parametric uncertainties are mass and moment of inertia, and the Cornell line of research also adopts this premise.

Another line of work is presented by Stanford University<sup>[19–21]</sup>. Cassinis *et al.*<sup>[19]</sup> introduced an adaptive convolutional neural network-based unscented Kalman filter for the pose estimation of uncooperative spacecraft. Park *et al.*<sup>[20]</sup> followed the same approach using a shared multi-scale feature encoder and multiple prediction heads that perform different tasks on a shared feature output, while Park *et al.*<sup>[21]</sup> also followed a comparative line similar to the Cornell approach presented in this manuscript, where the (to be proposed) deterministic approach is supple-

mented by an adaptive neural network-based unscented Kalman filter.

Cornell's Zhang *et al.* proposed an adaptive control strategy based on the full, nonlinear equations accounting for modeling uncertainties using an adaptive neural network amidst external disturbances<sup>[22]</sup>, where the Cornell approach stems from naval approaches proposed in 2020, called deterministic artificial intelligence<sup>[23]</sup>, which stated that the system dynamics constitute a feedforward control when paired with analytic trajectories; and when the dynamics are expressed in a canonical regression form, optimal feedback (in the two-norm sense) can aid control of spacecraft attitude. The method stems from the incremental development of a common nonlinear adaptive scheme offered by Slotine<sup>[24]</sup> for spacecraft attitude control, where elements of classical feedback were eliminated in 2020 and foremost applied to unmanned underwater robotics<sup>[25]</sup>. The burgeoning lineage of research continued in 2022 when Sandberg *et al.*<sup>[26]</sup> compared several trajectory-generation schemes and a nominal learning method based on the regression model, where applied torque is estimated by an enhanced Luengerberger observer. Very shortly afterwards, Raigoza<sup>[27]</sup> augmented Sandberg's trajectory generators with autonomous collision avoidance. In November 2022, Wilt examined efficacy in the face of simulated craft damage and environmental disturbances<sup>[28]</sup>. This sequel substantiates a short communication presenting significant findings that are part of the larger study of Slotine, Sands, Smeresky/Rizzo, Sandberg, Raigoza, and Wilt.

In prequel works<sup>[23–28]</sup>, the error convergence property is obtained using the proper design of the trajectory generation process. However, if the external disturbance makes the current state deviate from the trajectory, even if the system parameter is already converged to an accurate value, the trajectory will need to be re-calculated to fit the current state, so that the deterministic artificial intelligence can continue to drive the system using an optimal feedforward control signal.

As a result, provided the initial error between the current state and the current desired trajectory as well as inaccurate initial parameter value, the goal of the modified learning approach proposed in this manuscript is to guarantee the convergence to zero of both parameter error and the state error. This work focuses on the rotation rate control problem of a spacecraft and provided 2 ways of modification to the learning phase of the deterministic artificial intelligence algorithm and compared them with the original deterministic artificial intelligence using simulation in MATLAB<sup>®</sup>. Moreover, the modified method can be proved to make the error converge to zero using a similar way as how Slotine and Li<sup>[24]</sup> proved the stability of the non-linear system controlled by some specific feed-forward/feed-back controllers. That is, the Lyapunov candidate function is provided, and the time derivative of the candidate function can be proved to be negative with the proposed modified learning method.

**Main contribution of the study.** This paper provides 2 novel unknown parameter learning methods, that is, the time derivative of the vector of unknown, which are able to not just bound the error in parameter estimations but also the difference between the current system state and the desired state with respect to the planned trajectory. For the second method proposed, we will further show the convergence of parameter estimation error, as well as how this leads to the convergence of the state tracking error. The paper also discussed how the provided methods may fail to converge under certain conditions.

## 2. Materials and methods

### 2.1 Spacecraft rotation rate control

The spacecraft rotation rate control problem focuses on applying torque so that the rotation rate of a spacecraft converges to the desired value. The dynamic can be described by the Euler equation (displayed in equation (1)). Euler's moment equations can be parameterized in canonical regression form. This full form of the coupled,

nonlinear equations whose importance was highlighted by the research cited in the Introduction.

$$\tau = I\dot{\omega} + \omega \times I\omega = \underbrace{\begin{bmatrix} \dot{\omega}_x & \dot{\omega}_y - \omega_x\omega_z & \dot{\omega}_z + \omega_x\omega_y & -\omega_y\omega_z & \omega_y^2 - \omega_z^2 & \omega_y\omega_z \\ \omega_x\omega_z & \dot{\omega}_x + \omega_y\omega_z & \omega_z^2 - \omega_x^2 & \dot{\omega}_y & \dot{\omega}_z - \omega_x\omega_y & -\omega_x\omega_z \\ -\omega_x\omega_y & \omega_x^2 - \omega_y^2 & \dot{\omega}_x - \omega_y\omega_z & \omega_x\omega_y & \dot{\omega}_y + \omega_x\omega_z & \dot{\omega}_z \end{bmatrix}}_{\Phi} \underbrace{\begin{Bmatrix} I_{xx} \\ I_{xy} \\ I_{xz} \\ I_{yy} \\ I_{yz} \\ I_{zz} \end{Bmatrix}}_{\theta} \quad (1)$$

The matrix  $\Phi$  is the matrix of known, which is composed of the current state and the rate of the state ( $\omega$  and  $d\omega/dt$ ). The matrix  $\theta$  is the vector of the unknown, which is composed of system parameters, in this case, the moment of inertia. The way of formulation shows that it is possible to estimate the moment of inertia with the accurate measurement of the current state.

### 2.2 Original deterministic artificial intelligence control

The idea of deterministic artificial intelligence is that if the matrix of the unknown can be estimated and the desired trajectory of the state is given, the optimal control signal will be multiplying the desired matrix of known ( $\Phi_d$ ), which

includes the information of the current desired state, with the best guess of the parameter ( $\hat{\theta}$ ). This turns the system dynamic to equation (2).

$$\tau = \Phi\theta \rightarrow \tau_{applied} \equiv \Phi_d\hat{\theta} \quad (2)$$

However, the  $\hat{\theta}$  can be inaccurate or changed in the middle of the operation. Therefore, a learning approach should be provided so that the vector of the unknown can converge to an accurate value. The original learning approach in the space rotation rate control problem is described in equation (3-a) and (3-b), which is provided by Smeresky *et al.*<sup>[12]</sup> and is equation (12) in his publication.

$$\text{learned difference } d \equiv \theta - \hat{\theta} = \Phi^H(\tau_{applied} - \Phi\hat{\theta}) \quad (3-a)$$

$$\frac{d\hat{\theta}}{dt} = a * d \quad (3-b)$$

Where  $\tau_{applied}$  is the controller torque output, and the capital  $H$  means the pseudo inverse of a non-square matrix. In short, this provided a way to turn the difference between the applied torque and the expected torque into the

parameter error  $d$ , which should be a minimal square error estimation using the information in the current time stamp. Concerning the stability of the parameter estimation, the learning of the parameter is applied incrementally, and this can be done using a first order low pass filter to smoothen the learned difference.

Table 1. Symbols used in section 2.2

Variable	Physical meaning	Variable	Physical meaning
$\theta$	Vector of unknown	$I$	Moment of inertia
$\hat{\theta}$	Estimation on the unknown	$\omega$	Angular speed vector
$\Phi_d$	Matrix of known made by trajectory	$d$	Learned difference
$\Phi$	Matrix of known	$a$	Filter time constant
$\tau$	Applied torque		

Additionally, deterministic artificial intelligence requires a trajectory generation process to produce a trajectory that leads from the current state to the desired state. If the current state devi-

ates undesirably from the trajectory, it is better to update the trajectory, or the error of the state may accumulate. Please be aware that the desired state of the trajectory generation is not the desired state

of the controller, which follows the output of the trajectory generator by making the trajectory the desired state of the controller should follow. In this manuscript, all the “desired states” mentioned are the desired state for the controller, if not specifically noted.

The overall deterministic artificial intelligence can be expressed with the combination of control feedforward based on a desired trajectory as well as the current best estimation on the vector

of unknown and a “learning” mechanism that updates the vector of unknown until it goes to the actual value. **Figure 2** presents the deterministic artificial intelligence as a block diagram and shows the relationship between each component. In sections 2.3 and 2.4, the discussion focuses on the learning part of deterministic artificial intelligence and the goal is to learn the vector of unknown and decrease the tracking error at the same time.

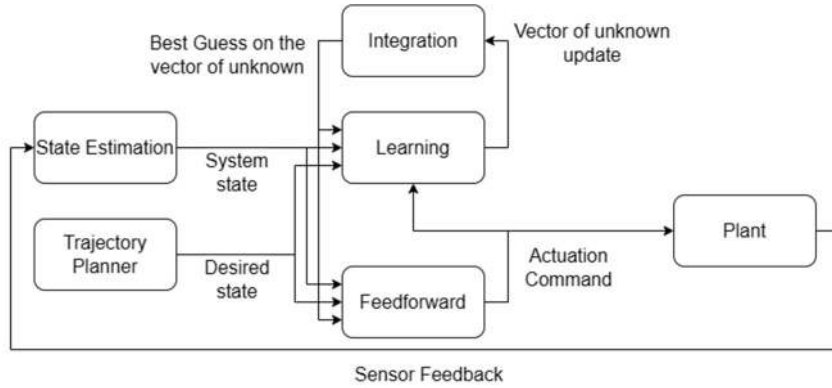


**Figure 2.** The block diagram for the deterministic artificial intelligence.

### 2.3 Modified learning method, a general version

The target of the modification is that if the learning approach can also guarantee to decrease the error in the current state when doing the parameter estimation, the chance of regenerating trajectory can be decreased because the error is kept from growing, which increases the robustness. In a general version of the modification, we consider all the systems that can be expressed in

$$\phi\theta + \phi\hat{\theta} = 0 \text{ where } \phi = \Phi_d - \Phi \text{ and } \theta = \theta - \hat{\theta} \quad (4)$$

Considering the Lyapunov candidate function described in equation (5), the function value must decrease to 0 if both  $\phi$  and  $\theta$  go to 0. If there is a parameter update approach  $\dot{\hat{\theta}}$  that makes the candidate function globally stable, it is very likely that the error of the state  $\phi$  goes to 0 together with  $\theta$ . Equation (7) shows that if  $\dot{\hat{\theta}}$  is taken in the form of equation (6), and considering

the regression form, as in equation (2), where the information of the current state is provided in the matrix of known. To study the error of the parameters and state, the error between the desired matrix of known and the current matrix of known is noted as  $\phi$ , and the error of the unknown vector is noted as  $\theta$ . Equation (2) can therefore be turned into equation (4). In this case, the goal becomes keeping both  $\phi$  and  $\theta$  bounded simultaneously using a modified learning method.

equation (4) and the time derivative of equation (4), the time derivative of the Lyapunov function will be negative semidefinite and leads to the global boundedness of the system as long as the matrix  $G$  is positive definitive.

$$V = \hat{\theta}^T \phi^T \phi \hat{\theta} + \theta^T \theta \quad (5)$$

$$\dot{\theta}^T = -\frac{d\hat{\theta}^T}{dt} = -\hat{\theta}^T \phi^T ((\Phi\dot{\Phi}^H)(\Phi^H + \Phi^T)^H + (\Phi^H + \Phi^T)^T G) \quad (6)$$

$$\frac{\dot{V}}{2} = [\hat{\theta}^T \phi^T \Phi \Phi^H + \hat{\theta}^T \Phi^H + \hat{\theta}^T \Phi^T] \phi \hat{\theta} = -\hat{\theta}^T \phi^T (\Phi^H + \Phi^T)^T G (\Phi^H + \Phi^T) \phi \hat{\theta} \leq 0 \quad (7)$$

However, this candidate function only provided the boundedness of  $\phi \hat{\theta}$  and  $\theta$ , and the derivation of equation (7) requires the matrix of known to be full rank. Furthermore, the convergence of  $\phi \hat{\theta}$ , even if it happens, is not equivalent to the convergence of the state even if the matrix of known is full rank. For example, for the target application in this manuscript (equation (1)), the rank of the matrix of known is at most 3, while the parameter number in the vector of unknown is 6, this makes the learning method provided unable to guarantee convergence. It is possible that when the unknown parameter converges to an accurate value and the state error still exists at the same time, the state error will not be going to be zero. This can be seen in equation (2) that when  $\hat{\theta} = \theta$ , the term  $\hat{\theta}^T \phi^T = \hat{\theta}^T (\Phi_d - \Phi)^T$

will always be 0. When  $\phi$  has a smaller rank than the number of unknowns, it is possible that  $\hat{\theta}^T \phi^T = 0$  when  $\phi$  is not zero.

Another concern of using this method is that the calculation of  $\dot{\Phi}$  is prone to noises and will cause latency in the real-time calculation because it requires the knowledge of the double derivative of the rotation rate, which generally requires special treatments like the smoothing process.

All in all, this version of modification will not guarantee the convergence of the state tracking error, so a closer inspection of the system dynamic, rather than a generalized “matrix of known times vector of unknown” formulation, may be necessary, and will be shown in section 2.4.

Table 2. Symbols used in section 2.3

Variable	Physical meaning	Variable	Physical meaning
$\phi$	Error in matrix of known	$V$	Lyapunov candidate function
$\theta$	Error in vector of unknown	$G$	Arbitrary positive definite matrix

## 2.4 Modified learning method, a specific version

To avoid the problem mentioned in section 2.3, a specific version of the modified learning method is provided for the rotation rate controller. The non-regression form of the system dynamic is considered in equation (8), and the modified learning method is provided in equation (10) which utilizes both the state error as well as parameter error. Also, the character “ $i$ ” means

the error in the inertia matrix in a  $3 \times 3$  form rather than in a  $1 \times 6$  unknown vector. The torque input to the system is slightly modified from  $\omega_d \times \hat{I} \omega_d$  to  $\omega_d \times \hat{I} \omega$ , which improves the global stability but won't affect the feed forward optimality in the deterministic artificial intelligence much when the state is very close to the desired value. (Or defined as applied torque (equation (8) in [12])).

$$I \dot{\omega} + \omega \times I \omega = \tau_{applied} \rightarrow \tau_{applied} \equiv \hat{I} \dot{\omega}_d + \omega_d \times \hat{I} \omega$$

Also, define  $i = I - \hat{I}$  and  $\omega' = \omega_d - \omega$  (8)

$$I \dot{\omega}' = -(\omega' \times I \omega_d - \omega' \times I \omega') + (i \dot{\omega}_d + \omega_d \times i \omega_d - \omega_d \times i \omega') = \omega' \times C + K \theta \quad (9)$$

$$\dot{\theta} = -\frac{d\hat{\theta}}{dt} = -Q \omega' - R \theta \quad (10)$$

The equation (8) is rearranged to equation (9), and the  $\theta$ , again, means the inertia in an unknown vector form. To prove the global con-

vergence of both state error  $\omega'$  and parameter error  $\theta$ , another Lyapunov function (equation (11)) is provided, which has a physical meaning

close to the square error of the whole system, where the state square error is weighted by the inertia. If the  $Q$  term in equation (10) is the transpose of the  $K$  term in equation (9), and the  $R$  term in equation (10) is positive definite, the Lyapunov function will be bounded globally, as shown in equation (12). About the parameter vector  $\theta$ , it is chosen based on equation (13), which is the least square estimation same as the equation (3-a), and the value is used for the modified learning method in equation (10).

$$\begin{aligned} \frac{\dot{V}}{2} &= \omega'^T I \dot{\omega}' + \theta^T \dot{\theta} = \omega'^T (\omega' \times C) + \theta^T (K^T - Q) \omega' - \theta^T R \theta \\ &= \theta^T (K^T - Q) \omega' - \theta^T R \theta = -\theta^T R \theta \leq 0 \end{aligned} \tag{12}$$

$$\theta = \Phi^H (\tau_{applied} - \Phi \hat{\theta}) \tag{13}$$

$$\frac{\dot{V}}{4} = \theta^T R K^T (\omega', \omega_d, \dot{\omega}_d) \omega' + \theta^T R^2 \theta \tag{14}$$

The discussion of convergence of tracking error can be based on the time integral of equation (10), as shown in equation (15). Since  $\theta$  is proven to be convergence, the right-hand side is now a constant and both terms at the right-hand side have finite value. As a result, it can be said that the term  $K^T \omega'$  goes to zero as time goes infinity, and the tracking error  $\omega'$  will be convergence as long as  $K^T$  always has a rank of 3.

Finally, the parameter vector  $\theta$  can be shown to converge in this case by applying Barbalat's lemma. Since the candidate function  $V$  is bounded, by equation (12) both tracking and estimation error is bounded, the desired trajectory has to be bounded, and  $K$  is a continuous function of  $\omega', \omega_d$ , and  $\dot{\omega}_d$ , it can be concluded that  $\frac{\dot{V}}{4}$  is bounded, which makes  $\dot{V}$  converges. As a result, the estimation error is convergence.

$$V(\omega', \theta) = \omega'^T I \omega' + \theta^T \theta \tag{11}$$

$$-\theta(0) = \int_0^\infty \dot{\theta} dt = - \int_0^\infty K^T \omega' dt - \int_0^\infty R \theta dt \tag{15}$$

The conclusion on the Lyapunov candidate is still based on the fact that the matrix of known has to be full rank, due to equation (13). Provided a full rank matrix of known, the candidate function will be driven to zero from any positive value. When the candidate function is zero, the tracking error and unknown vector estimation error will have to be zero as well.

Table 3. Symbols used in section 2.4

Variable	Physical meaning	Variable	Physical meaning
$i$	Error of inertia matrix	$C$	A term for simplifying equation (9)
$\omega'$	Error of angular velocity	$K$	A term for simplifying equation (9)
$Q$	Learning matrix for angular velocity error	$R$	Learning matrix for parameter estimation error

## 2.5 Simulation

The trajectory tracking of the rotation rate controller will be simulated. In the simulation, the trajectory is generated using arbitrary test torque, as shown in equation (16). The controller does not possess the test torque value, but instead receives a stream of desired rotation rate and the time derivative of the rotation rate. The idea is

that if the deterministic artificial intelligence can track the test trajectory, it should also be able to track any trajectory generated by another trajectory planner.

$$I \dot{\omega}_d + \omega_d \times I \omega_d = \tau_{test} \tag{16}$$

Two types of performance matrices are considered: norm ratio of the state error, and the

norm ratio of the parameter error, in equation (17). The result is plotted in section 3.

$$\begin{aligned} \text{State error norm ratio} &= \left( \frac{\|\omega'\|_2^2}{\|\omega_d\|_2^2} \right) \\ \text{Parameter error norm ratio} &= \ln \left( \frac{\|\theta'\|_2^2}{\|\theta\|_2^2} \right) \end{aligned} \quad (17)$$

### 3. Results

In this section, simulation results of the rotation rate problem (section 2.1) under different conditions are presented, and the performance of both types of modification (general version in section 2.3 and specific version in 2.4) is compared with the original deterministic artificial intelligence (section 2.2) learning approach.

#### 3.1 Performance comparison without the product of inertia

This case aims at testing the learning method when there is no product of inertia value in both the system’s true parameter and the initial estimation of the unknown vector, which can be seen as an indication of control design vulnerability to coupling effects in governing equation. If the products of inertia have to be zero, then in equation (1), the size of the matrix of known will be reduced from  $3 \times 6$  to  $3 \times 3$ , and the size of the vector of unknown will become  $3 \times 1$ . Intuitively speaking, we can have 3 equations and 3 unknowns in this case, making the unknown solvable using only the current information, as long as the matrix of known is full rank. The initial condition and the system parameters are listed in **Table 4**. The norm ratio of the state error and parameter error is shown in **Figure 3**. Also, the  $G$  in equation (7) and the  $R$  in equation (10) will be a scaler “ $r$ ” multiplied by a  $3 \times 3$  identity matrix, and this form of  $G$  and  $R$  will be used in all the cases presented in this manuscript.

**Table 4.** Initial condition for the simulation in section 3.1

Variable	Value	Variable	Value	Variable	Value
$I_{xx}$	1	$I_{yy}$	2	$I_{zz}$	3
$I_{xy}$	0.2	$I_{xz}$	0.3	$I_{yz}$	0.4
$\omega_{init,x}$	0.02	$\omega_{init,y}$	0.03	$\omega_{init,z}$	0.01
$\tau_{test,x}$	5	$\tau_{test,y}$	2	$\tau_{test,z}$	-2
r (specific)	3	r (general)	15	a	3

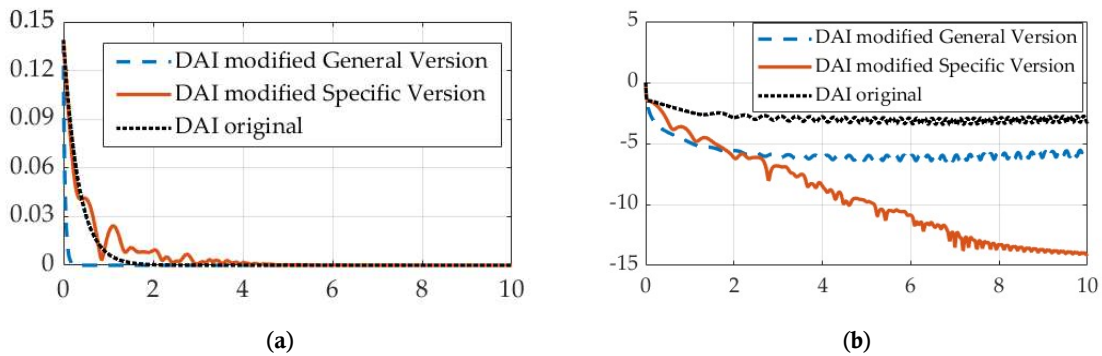


**Figure 3.** The convergence of the parameter error and state error. (a) Parameter error norm ratio on the ordinant versus time in seconds on the abscissa. (b) State error norm ratio on the ordinant versus time in seconds on the abscissa.

**Table 5.** Performance of inertia estimation and tracking errors

Figure of merit	Original method (prequels)	Proposed version general	Proposed version specific
Parameter error mean	0.0029	0.0058	0.0059
Parameter error deviation	0.0020	0.0038	0.0036
Mean tracking error	0.1709	0.0390	0.0076
Tracking error deviation	0.0862	0.0186	0.0083

### 3.2 Performance comparison with the product of inertia

This case is similar to section 3.1, but the product of inertia values in both the system’s true parameter and the initial estimation of the un-

known vector is not zero. The initial condition and the system parameters are listed in **Table 6**. The norm ratio of the state error and parameter error is shown in **Figure 4**.

**Table 6.** Initial condition for the simulation in section 3.2

Variable	Value	Variable	Value	Variable	Value
$I_{xx}$	1	$I_{yy}$	2	$I_{zz}$	1
$I_{xy}$	0.2	$I_{xz}$	0.3	$I_{yz}$	0.4
$\hat{I}_{xx,init}$	1.06	$\hat{I}_{yy,init}$	1.90	$\hat{I}_{zz,init}$	1.15
$\hat{I}_{xy,init}$	0.21	$\hat{I}_{xz,init}$	0.31	$\hat{I}_{yz,init}$	0.41
$\omega_{init,x}$	0.02	$\omega_{init,y}$	0.03	$\omega_{init,z}$	0.01
$\tau_{test,x}$	5	$\tau_{test,y}$	2	$\tau_{test,z}$	-2
$r$	3				

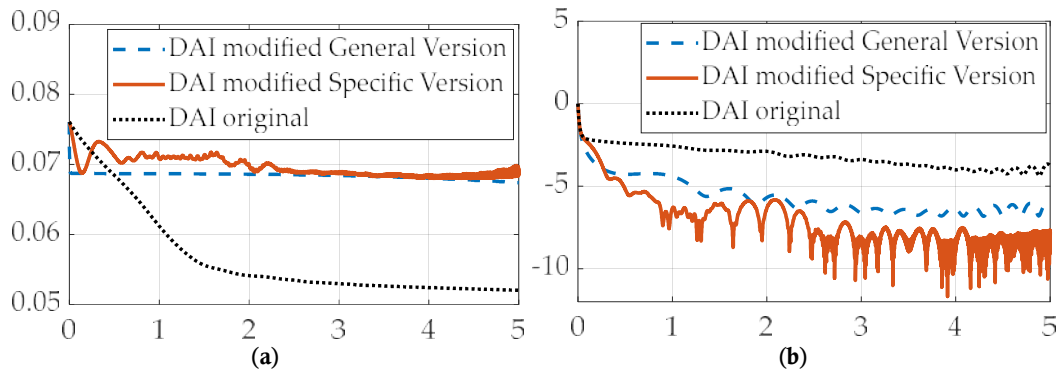


**Figure 4.** The convergence of the parameter error and state error. (a) Parameter error norm ratio on the ordinant versus time in seconds on the abscissa. (b) State error norm ratio on the ordinant versus time in seconds on the abscissa.

### 3.3 Performance comparison with different $r$ value

This case shows for the modified learning method (Specific Version) how the  $r$  value, which can be seen as the “magnitude” of the  $G$  in equa-

tion (7) and the  $R$  in equation (10), affects the final result. The initial condition and parameters used in this case are identical to case 3.2 and can be checked in **Table 6**, except for the  $r$  value.

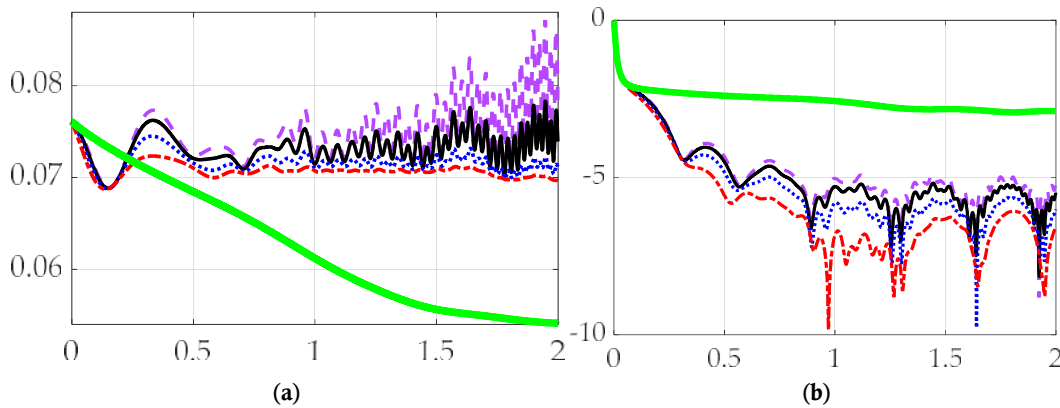


**Figure 5.** The convergence of the parameter error and state error. Original deterministic artificial intelligence is displayed by a thick, solid green line, dashed purple line displays  $r = 0.5$ , thin solid black line displays  $r = 1$ , dotted blue line displays  $r = 2$ , dot-dashed red line displays  $r = 4$ . (a) Parameter error norm ratio on the ordinant versus time in seconds on the abscissa. (b) State error norm ratio on the ordinant versus time in seconds on the abscissa.

**Table 7.** Convergence of inertia estimation and tracking errors

Figure of merit	Original method (prequels)	Modified with $r = 0.5$	Modified with $r = 1$	Modified with $r = 2$	Modified with $r = 4$
Parameter error mean	0.0247	0.0351	0.0348	0.0345	0.0341
Parameter error deviation	0.0124	0.0306	0.0272	0.0239	0.0217
Mean tracking error	-0.0401	-0.0033	-0.0033	-0.0033	-0.0034
Tracking error deviation	0.1761	0.0296	0.0246	0.0189	0.0143

## 4. Discussion

In sections 3.1 and 3.2, the modified learning method yields better state error convergence than the original method. For the specific version of the modified method, the final state error norm ratio is about 2 magnitudes smaller (rough order  $\times e^{-8}$  compared with  $\times e^{-3}$ ) than the original learning method, due to the data shown in both **Figures 3** and **4**.

In section 3.1, all the learning methods are able to make the parameter error converge to zero. This fits the expectation because in section 3.1 there is only 3 unknowns instead of 6. However, when the moment of inertia matrix contains the nonzero product of inertia, as has been done in section 3.2, the left part of **Figure 4** shows that the modified methods are not better than the original method.

**Table 8.** Percent performance enhancement: Convergence of inertia estimation and tracking errors

Figure of merit	Original method (prequels)	Proposed version general	Proposed version specific
Parameter error mean	0%	42%	53%
Parameter error deviation	0%	16%	100%
Mean tracking error	0%	-77%	-99%
Tracking error deviation	0%	-91%	-96%

In section 3.3, **Figure 5** shows that when the magnitude of  $R$  in equation (10) goes bigger, the convergence rate also increases. Because equation (12) states that the convergence rate of the Lya-

punov function (equation (11)) is only determined by the size of  $R$  and  $\theta$ , the result in section 3.3 is reasonable.

**Table 9.** Percent performance enhancement: Convergence of inertia estimation and tracking errors

Figure of merit	Original method (prequels)	Modified with $r = 0.5$	Modified with $r = 1$	Modified with $r = 2$	Modified with $r = 4$
Parameter error mean	0.00%	-42.11%	-40.89%	-39.68%	-38.06%
Parameter error deviation	0.00%	-146.77%	-119.35%	-92.74%	-75.00%
Mean tracking error	0.00%	91.77%	91.77%	91.77%	91.52%
Tracking error deviation	0.00%	83.19%	86.03%	89.27%	91.88%

From the convergence condition of errors in **Figures 3** and **4**, it can be concluded that the convergence trajectories of the specific version of the modified learning method are “bumpier” and contains more jitters and oscillations. This phenomenon may result from the way of  $\theta$  value determination provided in equation (13), which only consider the data in the current time stamp, and the indeterminate nature of equation (13), when the matrix of known is not full rank, makes the estimation of  $\theta$  very unstable.

It can be concluded that the specific version of the modified learning method can achieve the convergence of both parameter error and state error in the simulation done in this manuscript, especially when the matrix of known is full rank, which can increase the robustness of the rotation rate controller.

### 4.1 Recommended future work

From the parameter error data of the specific version of the modified method in **Figures 4** and **5**, the increasing jitters can be observed. The reason

for such instability after the convergence is unclear. It could result from the numerical instability of the chosen ODE solver and the options given to it, or the indeterminate way used for determining  $\theta$  value in equation (13).

Moreover, the property of the “general version of modified learning method” hasn’t been explored carefully because it is not suitable in this case by nature. Also, a better way of estimating  $\theta$  may improve the result of the modified learning method as well. Finally, a better way of choosing the  $G$  in equation (7) and the  $R$  in equation (10) is also an interesting topic.

## Conflict of interest

The authors declare no conflict of interest.

## References

- Johnson M. Space station robotic arms have a long reach [Internet]. Washington, DC: National Aeronautics and Space Administration; 2019 [updated 2022 Aug 13]. Available from: [https://www.nasa.gov/mission\\_pages/station/research/news/b4h-3rd/hh-robotic-arms-reach](https://www.nasa.gov/mission_pages/station/research/news/b4h-3rd/hh-robotic-arms-reach).
- Mahoney E. NASA seeks ideas for commercial uses of gateway [Internet]. Washington, DC: National Aeronautics and Space Administration; 2018 [updated 2018 Aug 25]. Available from: <https://www.nasa.gov/feature/nasa-seeks-ideas-for-commercial-uses-of-gateway>.
- NASA Image Use Policy [Internet]. Washington, DC: National Aeronautics and Space Administration. Available from: <https://gpm.nasa.gov/image-use-policy>.
- Bucchioni G, Innocenti M. Rendezvous in cis-lunar space near rectilinear halo orbit: Dynamics and control issues. *Aerospace* 2021; 8(3): 68. doi: 10.3390/aerospace8030068.
- Bando M, Namati H, Akiyama Y, Hokamoto S. Formation flying along libration point orbits using chattering attenuation sliding mode control. *Frontiers in Space Technologies* 2022; 3: 919932. doi: 10.3389/frspt.2022.919932.
- Colombi F, Colagrossi A, Lavagna M. Characterization of 6DOF natural and controlled relative dynamics in cislunar space. *Acta Astronautica* 2022; 196: 369–379. doi: 10.1016/j.actaastro.2021.01.017.
- Sands T. Flattening the curve of flexible space robotics. *Applied Sciences* 2022; 12(6): 2992. doi: 10.3390/app12062992.
- Sands T. Optimization provenance of whiplash compensation for flexible space robotics. *Aerospace* 2019; 6(9): 93. doi: 10.3390/aerospace6090093.
- Jones A. Chinese space station robot arm tests bring amazing views from orbit [Internet]. New York: Space.com; 2022 [updated 2022 Aug 9]. Available from: <https://www.space.com/china-space-station-wen-tian-robot-arm-test>.
- Jones A. See a large robotic arm “crawl” across China’s space station [Internet]. New York: Space.com; 2022 [published 2022 Feb 16]. Available from: <https://www.space.com/china-space-station-robot-arm-video>.
- Lafarge N, Miller D, Howell K, Linares R. Autonomous closed-loop guidance using reinforcement learning in a low-thrust, multi-body dynamical environment. *Acta Astronautica* 2021; 186: 1–23. doi: 10.1016/j.actaastro.2021.05.014.
- Albee K, Oestreich C, Specht C, *et al.* A robust observation, planning, and control pipeline for autonomous rendezvous with tumbling targets. *Frontiers in Robotics and AI* 2021; 8. doi: 10.3389/frobt.2021.641338.
- Mehta PM, Linares R. A new transformative framework for data assimilation and calibration of physical ionosphere-thermosphere models. *Space Weather* 2018; 16(18): 1086–1100. doi: 10.1029/2018SW001875.
- Oestreich CE, Linares R, Gondhalekar R. Autonomous six-degree-of-freedom spacecraft docking with rotating targets via reinforcement learning. *Journal of Aerospace Information Systems* 2021; 18(7): 417–428. doi: 10.2514/1.1010914.
- Avendaño M, Arnas D, Linares R, Lifson M. Efficient search of optimal flower constellations. *Acta Astronautica* 2021; 179: 290–295. doi: 10.1016/j.actaastro.2020.10.026.
- Arnas D, Lifson M, Linares R, Avendaño M. Definition of low earth orbit slotting architectures using 2D lattice flower constellations. *Advances in Space Research* 2021; 67(11): 3696–3711. doi: 10.1016/j.asr.2020.04.021.
- Oestreich C, Espinoza A, Todd J, *et al.* On-orbit inspection of an unknown, tumbling target using NASA’s Astrobe robotic free-flyers. In: 2021 IEEE/CVF Conference on Computer Vision and

- Pattern Recognition Workshops (CVPRW); 2021 Jun 20–25; Nashville. New York: Institute of Electrical and Electronics Engineers (IEEE); 2021. p. 2039–2047.
18. Roberts TG. Geosynchronous satellite maneuver classification and orbital pattern anomaly detection via supervised machine learning [Master's thesis]. Massachusetts (MA): Massachusetts Institute of Technology; 2021.
  19. Ekal M, Albee K, Coltin B, *et al.* Online information-aware motion planning with inertial parameter learning for robotic free-flyers. In: 2021 IEEE/RSJ International Conference on Intelligent Robots and Systems; 2021 Sep 27–Oct 1; Prague. New York: Institute of Electrical and Electronics Engineers (IEEE); 2021. p. 8766–8773. doi: 10.1109/IROS51168.2021.9636325.
  20. Cassinis LP, Park TH, Stacey N, *et al.* Leveraging neural network uncertainty in adaptive unscented Kalman Filter for spacecraft pose estimation. *Advances in Space Research* 2023; 71(12): 5061–5082. doi: 10.1016/j.asr.2023.02.021.
  21. Park TH, D'Amico S. Robust multi-task learning and online refinement for spacecraft pose estimation across domain gap. *Advances in Space Research* 2023. In Press. doi: 10.1016/j.asr.2023.03.036.
  22. Park TH, D'Amico S. Adaptive neural network-based unscented Kalman Filter for robust pose tracking of noncooperative spacecraft. New York: arXiv; 2022. doi: 10.48550/arXiv.2206.03796.
  23. Zhang K, Pan B. Control design of spacecraft autonomous rendezvous using nonlinear models with uncertainty. *Journal of Zhejiang University (Engineering Science)* 2022; 56(4): 833–842. doi: 10.3785/j.issn.1008-973X.2022.04.024.
  24. Smeresky B, Rizzo A, Sands T. Optimal learning and self-awareness versus PDI. *Algorithms* 2020; 13(1): 23. doi: 10.3390/a13010023.
  25. Slotine J, Li W. *Applied nonlinear control*. Wilmington, DE: Prentice-Hall, Inc.; 1991. p. 392–436.
  26. Sands T. Development of deterministic artificial intelligence for unmanned underwater vehicles (UUV). *Journal of Marine Science and Engineering* 2020; 8(8): 578. doi: 10.3390/jmse8080578.
  27. Sandberg A, Sands T. Autonomous trajectory generation algorithms for spacecraft slew maneuvers. *Aerospace* 2022; 9(3): 135. doi: 10.3390/aerospace9030135.
  28. Raigoza K, Sands T. Autonomous trajectory generation comparison for de-orbiting with multiple collision avoidance. *Sensors* 2022; 22(18): 7066. doi: 10.3390/s22187066.
  29. Wilt E, Sands T. Microsatellite uncertainty control using deterministic artificial intelligence. *Sensors* 2022; 22(22): 8723. doi: 10.3390/s22228723.

## Appendix A

The MATLAB® code used in this manuscript is pasted below. The program utilizes the ode45 solver to simulate the response of the overall system combining the controller and the controlled system.

```

clc; clear; close all
%% DAI Matrix Derivation
% =====
% Derive the matrix of known w.r.t. vector of unknown using symbolic
toolbox,
% and turn it into a matlab function.
% P is the matrix of known.
% th := [Ixx Ixy Ixz Iyy Iyz Izz]' is the vector of unknown.
% =====
syms fwx(t) fwy(t) fwz(t)
syms Ixx Ixy Ixz Iyy Iyz Izz real
syms wx wy wz dwx dwy dwz ddx dwy ddz real
w = [fwx;fwy;fwz];
wT = [fwx fwy fwz];
dw = diff(w,t);
ddw = diff(dw,t);
I = [Ixx Ixy Ixz; Ixy Iyy Iyz; Ixz Iyz Izz];
PhTh = I*dw + cross(w,I*w);
Peq = PhTh == 0;
[P, ~] = equationsToMatrix(Peq, [Ixx Ixy Ixz Iyy Iyz Izz]);
dP = diff(P,t);
sP = subs(P, [diff(diff(wT,t),t) diff(wT,t) fwx fwy fwz], [ddwx ddwy ddz dwx
dwy dwz wx wy wz]);
sdP = subs(dP, [diff(diff(wT,t),t) diff(wT,t) fwx fwy fwz], [ddwx ddwy ddz
dwx dwy dwz wx wy wz]);
sfP = symfun(sP, [wx wy wz dwx dwy dwz ddx ddz]);
sfdP = symfun(sdP, [wx wy wz dwx dwy dwz ddx ddz]);

%% Derive matrix K for the modified learning --- specific
% =====
% Derive the K matrix, mentioned in equation 9, used in specific learning,
% and turn it into a matlab function.
% i is the unknown vector error, i := I_real - I_estimate.
% w is the state error, w := w_desired - w_real.
% =====
syms wdx wdy wdz dwdx dwy ddz real
syms ixx ixy ixz iyy iyz izz real
w = [wdx;wyy;wz];
wd = [wdx;wdy;wdz];
dwd = [dwdx dwy ddz];
i = [ixx ixy ixz; ixy iyy iyz; ixz iyz izz];

```

```

Ki = i*dwd + cross(wd,i*wd) - cross(wd,i*w);
Keq = Ki == [0;0;0];
[K, sbz] = equationsToMatrix(Keq, [ixx ixy ixz iyy iyz izz]);
fK = symfun(K, [wx wy wz wdx wdy wdz dwdx dwdy dwdz]);

%% Simulation: ODE45
% =====
% Define simulation parameters and simulate
% =====
%
% ===== <Parameter definition> =====
p.J = [1 0.2 0.3; 0.2 2 0.4; 0.3 0.4 1]; % Example in section 3_2
p.dwd = [1 1 1]';
p.P = matlabFunction(sfP);
p.dP = matlabFunction(sfdP);
p.K = matlabFunction(fK);
p.G = 3*eye(6);
p.pinvTol = 1e-3;
Jt = [p.J(1,1);p.J(1,2);p.J(1,3);p.J(2,2);p.J(2,3);p.J(3,3)];
%
% ===== <Simulation time> =====
deltat = 0.01;
tfinal = 3;
t = 0:deltat:tfinal;% for evaluating solution
%
% ===== <Simulation: ODE45> =====
z0 = [1 0 0 0 0 0 0.02 0.03 0.01 1.06 0.21 0.31 1.90 0.41 1.15]'; % 3_2 0.08
0.08 004
options = odeset('absTol',1e-10,'relTol',1e-10);
% The simulation for the general version of modified learning method
[t_dai, z_dai] = ode45(@(t,z)DAI_modified_general(t,z,p), t, z0, options);
% The simulation for the specific version of modified learning method
[t_dmd, z_dmd] = ode45(@(t,z)DAI_modified_specific(t,z,p), t, z0, options);
% The simulation for the original version of learning method
[t_dor, z_dor] = ode45(@(t,z)DAI_original(t,z,p), t, z0, options);

%% Plot parameter estimations and state trajectories
figure()
plot(t_dai, z_dai(:,11),t_dai, z_dai(:,14),t_dai, z_dai(:,16))
legend('Ixx', 'Iyy', 'Izz');
title('Vector of unknown Estimation of DAI Modification General Version');
figure()
plot(t_dmd, z_dmd(:,11),t_dmd, z_dmd(:,14),t_dmd, z_dmd(:,16))
legend('Ixx', 'Iyy', 'Izz');
title('Vector of unknown Estimation of DAI Modification Specific Version');

```

```

figure()
plot(t_dor, z_dor(:,11),t_dor, z_dor(:,14),t_dor, z_dor(:,16))
legend('Ixx', 'Iyy', 'Izz');
title('Vector of unknown Estimation of Original DAI');
figure()
plot(t_dai, z_dai(:,7),t_dor, z_dor(:,7),t_dmd, z_dmd(:,7),t_dai, z_dai(:,10))
legend('Modified 1', 'Original', 'Modified 2', 'Desired');
title('Angular Velocity Tracking of DAI Modification General Version');
figure()
plot(t_dai, z_dai(:,6),t_dor, z_dor(:,6),t_dmd, z_dmd(:,6),t_dai, z_dai(:,9))
legend('Modified 1', 'Original', 'Modified 2', 'Desired');
title('Angular Velocity Tracking of DAI Modification Specific Version');
figure()
plot(t_dai, z_dai(:,5),t_dor, z_dor(:,5),t_dmd, z_dmd(:,5),t_dai, z_dai(:,8))
legend('Modified 1', 'Original', 'Modified 2', 'Desired');
title('Angular Velocity Tracking of Original DAI');

%% Analysis the norm rates
% inertia norm ratio: Equation 15
J_dai = z_dai(:,11:16);
J_dmd = z_dmd(:,11:16);
J_dor = z_dor(:,11:16);
n = length(t_dai);
nJ_dai = vecnorm(J_dai'-Jt*ones(1,n))/norm(Jt);
nJ_dmd = vecnorm(J_dmd'-Jt*ones(1,n))/norm(Jt);
nJ_dor = vecnorm(J_dor'-Jt*ones(1,n))/norm(Jt);
figure()
plot(t_dai, nJ_dai, t_dmd, nJ_dmd, t_dor, nJ_dor);
legend('DAI modified General Version', 'DAI modified Specific Version', 'DAI
original');
title('Convergence of the parameter error norm ratio');
xlabel('time (s)');
ylabel('Parameter error norm ratio');
% state error norm ratio: Equation 15
dw_dai = z_dai(:,5:7)-z_dai(:,8:10);
nw_dai = vecnorm(dw_dai')./vecnorm(z_dai(:,8:10));
dw_dmd = z_dmd(:,5:7)-z_dmd(:,8:10);
nw_dmd = vecnorm(dw_dmd')./vecnorm(z_dmd(:,8:10));
dw_dor = z_dor(:,5:7)-z_dor(:,8:10);
nw_dor = vecnorm(dw_dor')./vecnorm(z_dor(:,8:10));
figure()
plot(t_dai, log(nw_dai), t_dmd, log(nw_dmd), t_dor, log(nw_dor));
legend('DAI modified General Version', 'DAI modified Specific Version', 'DAI
original');
title('Convergence of the state error norm ratio');

```

```

xlabel('time (s)');
ylabel('State error norm ratio');

%% mean and deviation: Table 4
clc
% DAI modified General Version
ParamErrorMeanGeneral = mean(mean(J_dai-(Jt*ones(1,length(J_dai))))))
ParamErrorStdrGeneral = mean(std(J_dai-(Jt*ones(1,length(J_dai))))))
StateErrorMeanGeneral = mean(mean(dw_dai))
StateErrorStdrGeneral = mean(std(dw_dai))
% DAI modified Specific Version
ParamErrorMeanSpecific = mean(mean(J_dmd-(Jt*ones(1,length(J_dmd))))))
ParamErrorStdrSpecific = mean(std(J_dmd-(Jt*ones(1,length(J_dmd))))))
StateErrorMeanSpecific = mean(mean(dw_dmd))
StateErrorStdrSpecific = mean(std(dw_dmd))
% DAI Original
ParamErrorMeanOriginal = mean(mean(J_dor-(Jt*ones(1,length(J_dor))))))
ParamErrorStdrOriginal = mean(std(J_dor-(Jt*ones(1,length(J_dor))))))
StateErrorMeanOriginal = mean(mean(dw_dor))
StateErrorStdrOriginal = mean(std(dw_dor))

%% Test the performance of Specific Version Modified DAI in different G
% G = 0.5
p.G = 0.5*eye(6);
[t_dmd_h, z_dmd_h] = ode45(@(t,z)DAI_modified_specific(t,z,p), t, z0, options);
n = length(t_dmd_h);
J_dmd_h = z_dmd_h(:,11:16);
nJ_dmd_h = vecnorm(J_dmd_h'-Jt*ones(1,n))/norm(Jt);
dw_dmd_h = z_dmd_h(:,5:7)-z_dmd_h(:,8:10);
nw_dmd_h = vecnorm(dw_dmd_h')./vecnorm(z_dmd_h(:,8:10));
% G = 1
p.G = 1*eye(6);
[t_dmd_1, z_dmd_1] = ode45(@(t,z)DAI_modified_specific(t,z,p), t, z0, options);
J_dmd_1 = z_dmd_1(:,11:16);
nJ_dmd_1 = vecnorm(J_dmd_1'-Jt*ones(1,n))/norm(Jt);
dw_dmd_1 = z_dmd_1(:,5:7)-z_dmd_1(:,8:10);
nw_dmd_1 = vecnorm(dw_dmd_1')./vecnorm(z_dmd_1(:,8:10));
% G = 2
p.G = 2*eye(6);
[t_dmd_2, z_dmd_2] = ode45(@(t,z)DAI_modified_specific(t,z,p), t, z0, options);
J_dmd_2 = z_dmd_2(:,11:16);
nJ_dmd_2 = vecnorm(J_dmd_2'-Jt*ones(1,n))/norm(Jt);

```

```

dw_dmd_2 = z_dmd_2(:,5:7)-z_dmd_2(:,8:10);
nw_dmd_2 = vecnorm(dw_dmd_2')./vecnorm(z_dmd_2(:,8:10)');
% G = 4
p.G = 4*eye(6);
[t_dmd_4, z_dmd_4] = ode45(@(t,z)DAI_modified_specific(t,z,p), t, z0, op-
tions);
J_dmd_4 = z_dmd_4(:,11:16);
nJ_dmd_4 = vecnorm(J_dmd_4'-Jt*ones(1,n))/norm(Jt);
dw_dmd_4 = z_dmd_4(:,5:7)-z_dmd_4(:,8:10);
nw_dmd_4 = vecnorm(dw_dmd_4')./vecnorm(z_dmd_4(:,8:10)');
% Original
[t_dor, z_dor] = ode45(@(t,z)DAI_original(t,z,p), t, z0, options);
J_dor = z_dor(:,11:16);
nJ_dor = vecnorm(J_dor'-Jt*ones(1,n))/norm(Jt);
dw_dor = z_dor(:,5:7)-z_dor(:,8:10);
nw_dor = vecnorm(dw_dor')./vecnorm(z_dor(:,8:10)');
%
% Plot the result
rng = 200;
figure();
plot(t_dmd_h(1:rng), nJ_dmd_h(1:rng),...
      t_dmd_1(1:rng), nJ_dmd_1(1:rng),...
      t_dmd_2(1:rng), nJ_dmd_2(1:rng),...
      t_dmd_4(1:rng), nJ_dmd_4(1:rng),...
      t_dor(1:rng), nJ_dor(1:rng));
legend('DAI modified r = 0.5',...
       'DAI modified r = 1',...
       'DAI modified r = 2',...
       'DAI modified r = 4',...
       'DAI original');
title('Convergence of the parameter error norm ratio');
xlabel('time (s)');
ylabel('Parameter error norm ratio');
figure();
plot(t_dmd_h(1:rng), log(nw_dmd_h(1:rng)), ...
      t_dmd_1(1:rng), log(nw_dmd_1(1:rng)), ...
      t_dmd_2(1:rng), log(nw_dmd_2(1:rng)), ...
      t_dmd_4(1:rng), log(nw_dmd_4(1:rng)), ...
      t_dor(1:rng), log(nw_dor(1:rng)));
legend('DAI modified r = 0.5',...
       'DAI modified r = 1',...
       'DAI modified r = 2',...
       'DAI modified r = 4',...
       'DAI original');
title('Convergence of the state error norm ratio');

```

```

xlabel('time (s)');
ylabel('State error norm ratio');

%% mean and deviation: Table 6
% G = 0.5
ParamErrorMeanGHlf = mean(mean(J_dmd_h(1:rnge,)-(Jt*ones(1,rnge))))
ParamErrorStdrGHlf = mean(std(J_dmd_h(1:rnge,)-(Jt*ones(1,rnge))))
StateErrorMeanGHlf = mean(mean(dw_dmd_h(1:rnge,)))
StateErrorStdrGHlf = mean(std(dw_dmd_h(1:rnge,)))
% G = 1
ParamErrorMeanGOne = mean(mean(J_dmd_1(1:rnge,)-(Jt*ones(1,rnge))))
ParamErrorStdrGOne = mean(std(J_dmd_1(1:rnge,)-(Jt*ones(1,rnge))))
StateErrorMeanGOne = mean(mean(dw_dmd_1(1:rnge,)))
StateErrorStdrGOne = mean(std(dw_dmd_1(1:rnge,)))
% G = 2
ParamErrorMeanGTwo = mean(mean(J_dmd_2(1:rnge,)-(Jt*ones(1,rnge))))
ParamErrorStdrGTwo = mean(std(J_dmd_2(1:rnge,)-(Jt*ones(1,rnge))))
StateErrorMeanGTwo = mean(mean(dw_dmd_2(1:rnge,)))
StateErrorStdrGTwo = mean(std(dw_dmd_2(1:rnge,)))
% G = 4
ParamErrorMeanGFor = mean(mean(J_dmd_4(1:rnge,)-(Jt*ones(1,rnge))))
ParamErrorStdrGFor = mean(std(J_dmd_4(1:rnge,)-(Jt*ones(1,rnge))))
StateErrorMeanGFor = mean(mean(dw_dmd_4(1:rnge,)))
StateErrorStdrGFor = mean(std(dw_dmd_4(1:rnge,)))
% Original DAI
ParamErrorMeanOrig = mean(mean(J_dor(1:rnge,)-(Jt*ones(1,rnge))))
ParamErrorStdrOrig = mean(std(J_dor(1:rnge,)-(Jt*ones(1,rnge))))
StateErrorMeanOrig = mean(mean(dw_dor(1:rnge,)))
StateErrorStdrOrig = mean(std(dw_dor(1:rnge,)))

%% Function
function zdot = DAI_modified_general(t, z, p)
    % Orientation of the rigid body as quaternion
    q = z(1:4);
    % Angular velocity
    w = z(5:7);
    % Desired velocity
    wd = z(8:10);
    % Vector of unknown: Inertia
    th = z(11:16); % theta hat
    Jh = [th(1) th(2) th(3); th(2) th(4) th(5); th(3) th(5) th(6)];
    % Generate trajectory to be followed
    [sdwd,sddwd] = traj_gen(t,wd,p);
    % Generate feed forward control torque
    tau = Jh*sdwd + cross(wd', Jh*wd);

```

```

% Update the dynamic of the system
dw = p.J\(\tau-cross(w', p.J*w');
dq = 0.5*quatmultiply([0 w'],q');
% Update the parameter estimation
ddw = [0;0;0];
% Matrix of known w.r.t. desired angular velocity
Pd
=
p.P(wd(1),wd(2),wd(3),sdwd(1),sdwd(2),sdwd(3),sddwd(1),sddwd(2),sddwd(3));
% Matrix of known w.r.t. actual angular velocity
P = p.P(w(1),w(2),w(3),dw(1),dw(2),dw(3),0,0,0);
% Time derivative of the Matrix of known w.r.t. actual angular velocity
dP = p.dP(w(1),w(2),w(3),dw(1),dw(2),dw(3),ddw(1),ddw(2),ddw(3));
% Equation 6: General version of modified learning in DAI
ph = Pd-P;
A = dP*pinv(P,p.pinvTol)*pinv(P' + pinv(P,p.pinvTol),p.pinvTol);
B = (P' + pinv(P,p.pinvTol))*p.G;
dth = (th'*ph*(A+B));
% Print simulation time every 1 second
if abs(t-round(t)) < 0.001
    disp(t)
end
zdot = [dq';dw';sdwd';dth];
end

```

```

function zdot = DAI_modified_specific(t, z, p)
% Orientation of the rigid body as quaternion
q = z(1:4);
% Angular velocity
w = z(5:7);
% Desired velocity
wd = z(8:10);
% Vector of unknown: Inertia
th = z(11:16); % theta hat
Jh = [th(1) th(2) th(3); th(2) th(4) th(5); th(3) th(5) th(6)];
% Generate trajectory to be followed
[sdwd,~] = traj_gen(t,wd,p);
% Generate feed forward control torque: Equation 8
tau = Jh*sdwd + cross(wd', Jh*w');
% Update the dynamic of the system
dw = p.J\(\tau-cross(w', p.J*w');
dq = 0.5*quatmultiply([0 w'],q');
% Update the parameter estimation
P = p.P(w(1),w(2),w(3),dw(1),dw(2),dw(3),0,0,0);
% Equation 9/12: Specific version of modified learning in DAI
ew = wd-w;

```

```

K = p.K(ew(1),ew(2),ew(3),wd(1),wd(2),wd(3),sdwd(1),sdwd(2),sdwd(3));
Dth = pinv(P,p.pinvTol)*(tau-P*th);
dth = K'*ew+p.G*Dth;
% Monitor the Lyapunov Candidate function to see if it is decreasing
% TDth = [p.J(1,1);p.J(1,2);p.J(1,3);p.J(2,2);p.J(2,3);p.J(3,3)]-th;
% V = ew'*p.J*ew+TDth*TDth
zdot = [dq';dw;sdwd;dth];
end

```

```

function zdot = DAI_original(t, z, p)
% Orientation of the rigid body as quaternion
q = z(1:4);
% Angular velocity
w = z(5:7);
% Desired velocity
wd = z(8:10);
% Vector of unknown: Inertia
th = z(11:16); % theta hat
Jh = [th(1) th(2) th(3); th(2) th(4) th(5); th(3) th(5) th(6)];
% Generate trajectory to be followed
[sdwd,~] = traj_gen(t,wd,p);
% Generate feed forward control torque
tau = Jh*sdwd + cross(wd', Jh*wd)';
% Update the dynamic of the system
dw = p.J\(\tau-cross(w', p.J*w));
dq = 0.5*quatmultiply([0 w'],q);
% Update the parameter estimation: Equation 3-a, 3-b
P = p.P(w(1),w(2),w(3),dw(1),dw(2),dw(3),0,0,0);
dth = 1.5*pinv(P,p.pinvTol)*(tau-P*th);
zdot = [dq';dw;sdwd;dth];
end

```

```

function [dwd,ddwd] = traj_gen(t,wd,p)
tau = [5;2;-2];
if t>7
tau = [0;0;0];
end
dwd = p.J\(\tau-cross(wd', p.J*wd)');
ddwd = [0;0;0];
end

```

# Statistical analysis of a Tagore song based on Raga Kafi

Soubhik Chakraborty\*, Prerna Singh

Department of Mathematics, Birla Institute of Technology, Mesra, Ranchi 835215, India. E-mail: soubhikc@yahoo.co.in

## ARTICLE INFO

Received: 19 February 2023  
Accepted: 17 March 2023  
Available online: 25 April 2023

<http://dx.doi.org/10.59400/jam.v1i1.85>

Copyright © 2023 Author(s).

Journal of AppliedMath is published by Academic Publishing Pte. Ltd. This article is licensed under the Creative Commons Attribution-NonCommercial 4.0 International License (CC BY-NC 4.0).  
<https://creativecommons.org/licenses/by-nc/4.0/>

**ABSTRACT:** *Rabindra Sangeet* or Tagore songs encompass a wide variety of human emotions. Most of these songs are based on Hindustani ragas. Kafi is a joyful raga and therefore could be helpful to combat stress. We are motivated to analyse a popular Tagore song, namely, *Momo Chitte*, which is based on this raga. Statistical analysis compares two phases of 30 s each of a vocal recording of this song. Several statistical features are considered including note duration, inter onset interval, rate of change of pitch, statistical parameterization of melody and rhythm in addition to analysis of spectrogram and pitch profile. The experimental results are encouraging.

**KEYWORDS:** note duration; inter onset interval; rate of change of pitch; statistical parameterization of melody and rhythm; spectrogram

## 1. Introduction

*Rabindra Sangeet* or Tagore songs are songs written and composed by the great laureate of literature, poet Gurudev Rabindranath Tagore. He was the first Nobel laureate from the Asian origin who received the Nobel prize in literature in 1913. While the lyrics of all these songs are credited to Tagore, there are a few exceptions in which the tunes are composed by someone else, e.g., Pankaj Mallick composed the tune of the Tagore song *Diner Sheshe Ghumer Deshe* and the tune was highly appreciated by Tagore.

Indian classical music has two forms—Hindustani and Carnatic (or North Indian and South Indian classical music respectively). In either form, the central focus is the raga which is a melodic structure with fixed notes and a set of rules that characterises a particular mood which is conveyed by performance.

*Rabindra Sangeet* has a great impact on human emotion. Kafi, being a joyful raga, motivated us to study the statistical properties of a *Rabindra Sangeet*, namely, *Momo Chitte* based on this raga. This song would be used in subsequent studies in music intervention for therapeutic purpose to combat

stress. Statistical analysis compares two phases of 30 s each of a vocal recording of this song. Several statistical features are considered including note duration, inter onset interval, rate of change of pitch, statistical parameterization of melody and rhythm in addition to analysis of spectrogram and pitch profile.

## 2. State of the art

Rabindranath Tagore received his initial training in music from Jyotirindranath, his elder brother. Jyotirindranath was an accomplished classical musician specializing in dhrupad, dhamar and khayal. Since the days of initial training, Tagore started composing verses and attempted to place them in the melodic framework of the Ragas. That was how *Rabindra Sangeet* or Tagore Songs germinated<sup>[1]</sup>.

Musical composition and background history of the song:

Parjaay: Bichitro (6)

Taal: Kashmiri Khemta

Raag: Kafi

Written on: 1910

Collection: Arupratan, Raja, Shrabon-gatha

Swarabitan: 42 (Arupratan)

Notation by: Surendranath Bandopadhyay

Lyrics:

Mamo chitte niti nritye ke je naache  
 Taata thoi thoi, taata thoi thoi, taata thoi thoi,  
 Taari sange ki mridange sada baaje  
 Taata thoi thoi, taata thoi thoi, taata thoi thoi.  
 Haasi kaanna hira paanna dole bhaale,  
 Knaape chhande bhaalomondo taale taale,  
 Naache janmo naache mrityu paachhe paachhe,  
 Taata thoi thoi, taata thoi thoi, taata thoi thoi.  
 Ki anondo, ki anondo, ki anondo  
 Dibaraatri naache mukti naache bandho  
 Se taronge chhuti range paachhe paachhe  
 Taata thoi thoi, taata thoi thoi, taata thoi thoi.

Further literature on the song lyrics of *Momo Chitte* and its background information can be found from the website<sup>[2]</sup>. An English translation of this song by Anjan Ganguly is given in the Appendix.

Music researchers have been using statistics for studying the musical patterns. Beran's book<sup>[3]</sup> gives an account of the applications of statistics in Western Art Music (WAM) while the book by Chakraborty *et al.*<sup>[4]</sup> provides the same in Hindustani music. The book by Jairazbhoy<sup>[5]</sup> may be consulted for further literature on Hindustani ragas. See also the book of Bor *et al.*<sup>[6]</sup>.

### 3. Methodology

#### 3.1 Notes duration

The length of time for which a note is played in any music is called the note duration. It can be understood more precisely by saying that it is the difference between the time of departure and time of arrival of a note. Note duration analysis is important to depict the restfulness or restlessness in the concerned regions in the musical piece where there is greater stay or lesser stay respectively on the notes.

#### 3.2 Inter onset interval (IOI)

IOI is the difference in arrival times of two successive notes. IOI analysis is necessary to depict rhythm. Equal peaks in the IOI graph indicate

that the notes are coming periodically and hence are in rhythm. If the mean IOI is less, it implies that notes have arrived more rapidly in the recording. If the standard deviation of IOI is less, it implies there is more rhythm in the notes.

#### 3.3 Pitch velocity

Pitch velocity is the rate of change of pitch with respect to time obtained by dividing the absolute value of pitch difference of two successive notes by the corresponding inter onset interval (IOI).

#### 3.4 Statistical parameterization

The structural attributes of a musical phrase can be efficiently described by using the designed statistical parameterization approach<sup>[7]</sup>. The method is mathematically valid and it gives precise results. In what follows,  $P_1$ ,  $P_2$  and  $P_3$  measure melody while  $P_4$  and  $P_5$  measure rhythm. Let  $P_1$  be the difference between weighted average note pitch and the pitch of the lowest note of a musical phrase and can be defined as:

$$P_1 = \frac{\sum_{i=1}^N p_i d_i}{\sum_{i=1}^N d_i} - \text{Min}(p_i)$$

where  $p_i$  denotes the pitch (at the onset) of the  $i$ -th note and  $d_i$  denotes the duration of the  $i$ -th note (departure time of the  $i$ -th note-onset time of the  $i$ -th note),  $N$  denotes the number of notes in a musical phrase.

Let  $P_2$  be the difference between the pitch of the highest and the lowest note of a musical phrase and can be defined as:

$$P_2 = \text{Max}(p_i) - \text{Min}(p_i)$$

Let  $P_3$  be the average absolute difference of the pitches of subsequent notes and can be defined as:

$$P_3 = \frac{1}{N-1} \sum_{i=1}^{N-1} |p_i - p_{i-1}|$$

Let  $P_4$  be the duration of the longest note of a musical phrase and can be defined as:

$$P_4 = \text{Max}(d_i)$$

Let  $P_5$  be the average note duration and can be defined as:

$$P_5 = \frac{1}{N} \sum_{i=1}^N d_i$$

### 3.5 Spectrogram

A spectrogram is a visual representation of voice (in our case) graphically in which a two-dimensional spectrogram shows frequency on one axis with respect to time on the other axis and in 3-D spectrogram depicts one of the axis representing amplitude of sound. By the use of spectrogram, it is easy to analyse the intensity of different sounds like music, sonar, radar, speech processing, and linguistics, by varying the colour or brightness in the image.

### 3.6 Pitch profile

Pitch is the perceived fundamental frequency which determines the shrillness or hoarseness of sound. Musical notes are characterised by their pitch and pitch class. The pitch profile provides the pattern in the note progression in the musical piece.

## 4. Experimental results

Figures 1 and 2 give the note duration in seconds for the first 30 s and the next 30 s respectively of the recording.

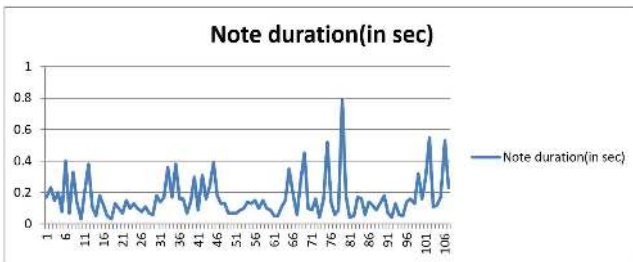


Figure 1. Note duration graph for the first 30 s. Mean note duration = 0.157029703 s, SD (standard deviation) note duration = 0.118106262 s.

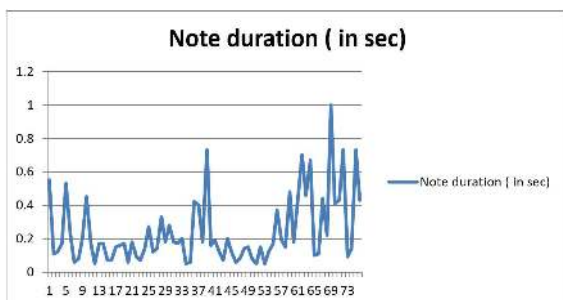


Figure 2. Note duration graph for the next 30 s. Mean note duration = 0.240789474 s, SD (standard deviation) Note duration = 0.202239219 s.

Figures 3 and 4 give the IOI for the first 30 s and the next 30 s respectively.



Figure 3. IOI graph for the first 30 s. Mean IOI = 0.289705882 s, SD (standard deviation) IOI = 0.175245796 s.

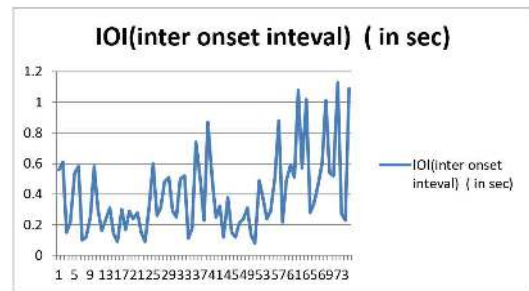


Figure 4. IOI graph for the next 30 s. Mean IOI = 0.395333333 s, SD (standard deviation) = 0.257814795 s.

Figures 5 and 6 give the pitch velocity for the first 30 s and the next 30 s respectively.

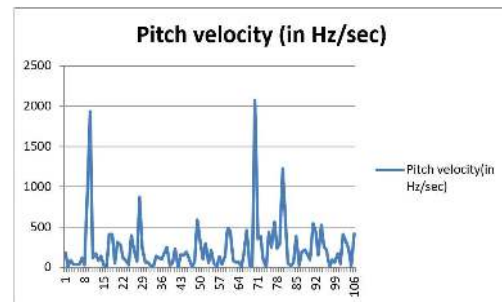


Figure 5. Graph showing pitch velocity for the first 30 s. Mean of pitch velocity = 234.0169307 Hz/s, SD (standard deviation) of pitch velocity = 331.5644264 Hz/s.

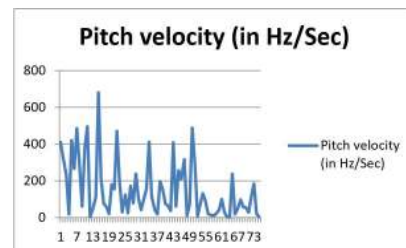


Figure 6. Graph showing pitch velocity for the next 30 s. Mean of pitch velocity = 150.4494667 Hz/s, SD (standard deviation) of pitch velocity = 152.4132939 Hz/s.

**Table 1** gives the values of statistical parameters  $P_1$ ,  $P_2$ ,  $P_3$ ,  $P_4$  and  $P_5$  for the first 30 s and next 30 s of the recording.

**Table 1.** Comparison of statistical parameters  $P_1$ ,  $P_2$ ,  $P_3$ ,  $P_4$  and  $P_5$  for the first and next 30 s.

	$P_1$	$P_2$	$P_3$	$P_4$	$P_5$
First 30 s	56.797	233.94	48.003	0.79	0.157
Next 30 s	55.668	230.06	150.449	1	0.241

Spectrogram analysis: The spectrogram for the first 30 s and the second 30 s are given in **Figures 7 and 8**, respectively.

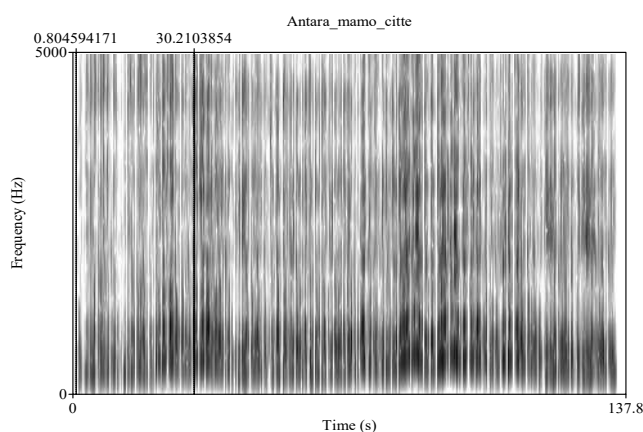


**Figure 7.** Spectrogram of Tagore song *Momo Chitte* for first 30 s.

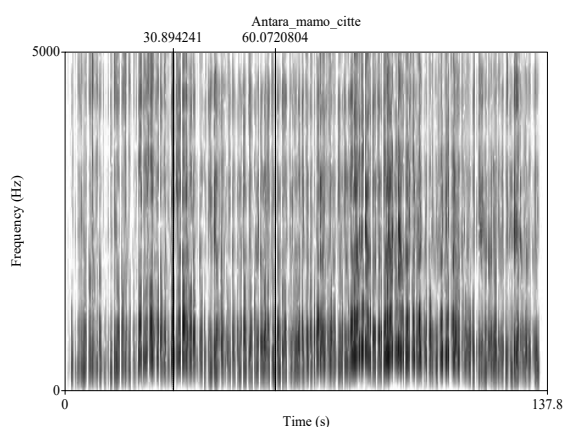


**Figure 8.** Spectrogram of Tagore song *Momo Chitte* for next 30 s.

Pitch profile: The pitch profile for the first 30 s and the second 30 s are given in **Figures 9 and 10**, respectively.

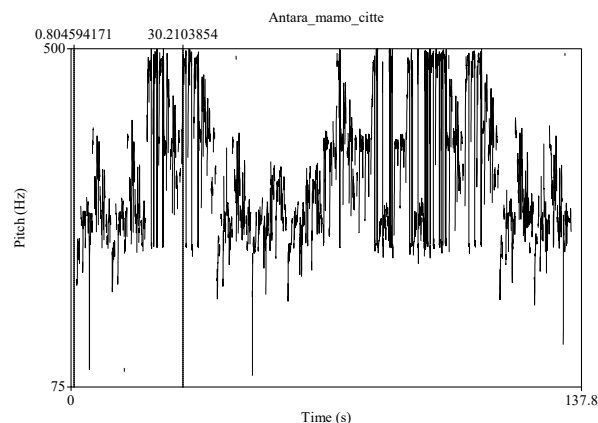


**Figure 9.** Pitch profile of Tagore song *Momo Chitte* for first 30 s.

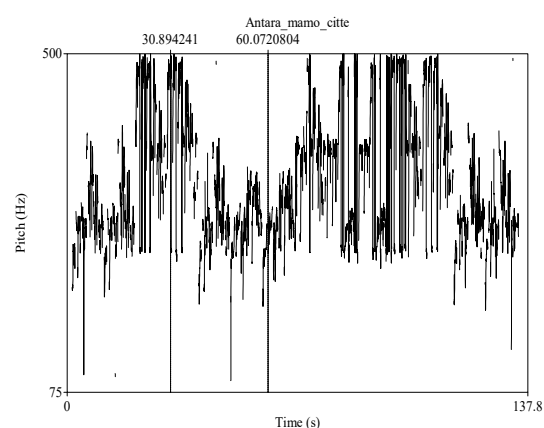


**Figure 10.** Pitch profile of Tagore song *Momo Chitte* for second 30 s.

## 5. Discussion

From **Figures 1 and 2**, it is clear that the peaks of note duration are greater and higher in the second 30 s of the recording implying more restfulness or stay on the notes in the second 30 s as compared to the first 30 s. The mean note duration is more in the second 30 s. However, the standard deviation is less in the first 30 s implying less variation in the duration times of the notes in the first 30 s.

From **Figures 3 and 4**, it is evident that notes are coming more rapidly and also have more rhythm in the first 30 s as compared to the second 30 s of the recording which is also numerically endorsed by the fact that both the mean and standard deviation of IOI is less in the first 30 s.

From **Figures 5 and 6**, the rate of change of pitch is less in the second 30 s of the recording as

compared to the first 30 s. Both the mean and standard deviation of the pitch velocity is lesser in the second 30 s.

From **Table 1**, the parameters  $P_1$  and  $P_2$  are close in the first 30 s and second 30 s, but the parameter  $P_3$  is more in the second 30 s. It is interesting to observe that, while the rate of change of pitch is less in the second 30 s, the average pitch difference between successive notes is more. Also, the parameters  $P_4$  and  $P_5$  are more in the second 30 s depicting that both the maximum and the average note duration are more in the second 30 s.

From **Figures 7 and 8**, it is evident that the intensity is more in the first 30 s. Also, there is varying intensity in the first 30 s as compared to the second 30 s.

From **Figures 9 and 10**, we notice the contrasting pitch profile in the first 30 s showing an upward trend as compared to that of the second 30 s showing a downward trend of note progression.

## 6. Conclusion

We conclude that:

1) There is more restfulness or stay on the notes in the second 30 s but less variation in the duration times of the notes in the first 30 s.

2) Notes are coming more rapidly and also have more rhythm in the first 30 s as compared to the second 30 s.

3) The rate of change of pitch is less in the second 30 s of the recording with lesser standard deviation as compared to the first 30 s.

4) The parameters  $P_1$  and  $P_2$  are close in the first 30 s and second 30 s, but the parameter  $P_3$  is more in the second 30 s. It is interesting to observe that, while the rate of change of pitch is less in the second 30 s, the average pitch difference between successive notes is more. Also, the parameters  $P_4$  and  $P_5$  are more in the second 30 s depicting that both the maximum and the average note duration are more in the second 30 s.

5) The intensity is more in the first 30 s. Also, there is varying intensity in the first 30 s as compared to the second 30 s.

6) The pitch profile in the first 30 s shows an upward trend as compared to that of the second 30 s showing a downward trend of note progression.

## Author contributions

Conceptualization, SC; methodology, SC; software, SC and PS; validation, SC and PS; formal analysis, PS; investigation, SC and PS; resources, PS; data curation, PS; writing—original draft preparation, SC and PS; writing—review and editing, SC; visualization, SC; supervision, SC; project administration, SC; funding acquisition, SC. All authors have read and agreed to the published version of the manuscript.

## Acknowledgment

The authors would like to thank IDEA: Technology Innovation Hub @ Indian Statistical Institute, Kolkata for sponsoring this research.

It is also a pleasure to thank Antara Sengupta for sharing her vocal recording of the Tagore song *Momo Chitte* for our research.

## Conflict of interest

The authors declare no conflict of interest.

## References

1. Roy K. Even with Hindustani classical music Tagore was an avant-garde [Internet]. Kolkata: the SpaceInk; 2020. Available from: <https://thespace.ink/cover-story/rabindra-sangeet-and-hindustani-classical-music/>.
2. Lyric and background history of song Mamo Chitte Niti Nritye [Internet]. Available from: <https://www.geetabitan.com/lyrics/M/mamo-chitte-niti-nritte-lyric.html>.
3. Beran J. Statistics in musicology. 1<sup>st</sup> ed. New York: Chapman and Hall/CRC; 2003.
4. Chakraborty S, Mazzola G, Tewari S, Patra M. Computational musicology in Hindustani music. Cham: Springer Cham; 2014.
5. Jairazbhoy NA. The rags of North Indian music: Their structure and evolution. 2<sup>nd</sup> ed. Mumbai: Popular Prakashan; 2011.

6. Bor J, Rao S, Meer WV, Harvey J. The raga guide: A survey of 74 Hindustani ragas. Charlottesville: Nimbus Records; 1999.
7. Kostek B. Perception based data processing in acoustics: Applications to music information retrieval and sychophysiology of hearing. Heidelberg: Springer Berlin; 2005.
8. English translation of song Mamo Chitte Niti Nritye [Internet]. Available from: <https://www.geetabitan.com/lyrics/rs-m/mamo-chitte-niti-nritte-english-translation.html>.

## Appendix

English translation of the song *Momo Chitte*<sup>[8]</sup>  
by Anjan Ganguly.

I wonder, who is that dances in my mind

The eternal dance, rhythmically.

I wonder, how well my soul and body respond

To the meter of the 'MRIDANGA',

The eternal dance, rhythmically.

Swings smile and tears upon the temple jewel-like

Good and the evil pulsate with the rhythm

Keenly follow life and death, dancing along

The eternal dance, rhythmically.

O, what a delight, what a delight,

Confinement and liberation dance alongside day and  
night,

I follow the wave closely, enjoy running behind it

The eternal dance, rhythmically.

# Machine learning in coal and gas outburst prediction

Peng Ji\*, Shiliang Shi

Hunan University of Science and Technology, Xiangtan 411199, Hunan Province, China. E-mail: [jipengem@gmail.com](mailto:jipengem@gmail.com)

## ARTICLE INFO

Received: 5 March 2023  
Accepted: 1 April 2023  
Available online: 27 April 2023

<http://dx.doi.org/10.59400/jam.v1i1.74>

Copyright © 2023 Author(s).

*Journal of AppliedMath* is published by Academic Publishing Pte. Ltd. This article is licensed under the Creative Commons Attribution-NonCommercial 4.0 International License (CC BY-NC 4.0).  
<https://creativecommons.org/licenses/by-nc/4.0/>

**ABSTRACT:** Artificial intelligence is flourishing, and its research achievements are being extensively applied across various industries. In the field of predicting coal and gas outbursts, methods such as machine learning and deep learning have been widely explored, resulting in accurate prediction accuracy and excellent predictive effects. This has significantly improved the safety of coal mine underground operations.

**KEYWORDS:** machine learning; coal and gas outburst prediction; deep learning; artificial intelligence; application

## 1. Introduction and observation

During the stage of establishing an indicator system for predicting coal and gas outburst, Wu *et al.*<sup>[1]</sup> have employed machine learning methods such as decision trees and random forests to identify and select the influencing factors of coal and gas outbursts. They evaluate the importance of each factor and choose more effective predictive indicators based on their importance, using these scientific algorithms from the beginning to move towards accurate predictions.

Furthermore, in the process of handling the collected raw data for coal and gas outburst indicators, scientific machine learning methods are also applied. Methods such as Seasonal and Trend decomposition using Loess (STL) and wavelet denoising are utilized for regularity processing of time series data and noise reduction, achieving preprocessing and in-depth processing of the data. For example, Zhang *et al.*<sup>[2]</sup> use wavelet denoising to denoise the collected coal mine gas raw data. Such processing enables researchers to observe potential hazards through the regularity exhibited by the data, thereby preparing for further prediction work.

On this basis, some machine learning models that are consistent with the prediction needs of coal and gas outbursts are gradually being explored in coal and gas outburst prediction research<sup>[3]</sup>, such as Back Propagation neural network (BP), Support Vector Machine algorithm (SVM), Long Short-Term Memory network (LSTM), Bi-directional Long Short-Term Memory network (Bi-LSTM), and Artificial Immune Algorithm (AIA)<sup>[4]</sup>, etc. At the same time, based on the practical needs of coal and gas outburst prediction, these methods have been optimized accordingly, such as Xue *et al.*<sup>[5]</sup> using a genetic algorithm to optimize support vector machine, and Peng *et al.*<sup>[6]</sup> using particle swarm optimization algorithm to optimize the immune algorithm. Two or more models have complementary performance, forming some combination models, which significantly improve prediction accuracy and prediction effectiveness<sup>[7]</sup>.

Through active exploration of the application of machine learning methods in coal and gas outburst prediction, coal mine safety technology has also been developed and iterated in the prevention and control of coal and gas outburst<sup>[8,9]</sup>. It has demonstrated beneficial effects and improved the

level of coal mine safety. With the current trend of mining automation and intelligence, more machine learning-based coal and gas outburst prediction methods with better performance can be explored.

## Acknowledgments

This work is financially supported by the National Natural Science Foundation of China (Nos. 51974120 and 52274196). The author thanks the mentor Professor Shiliang Shi for his careful guidance and critical reviews.

## Conflict of interest

The authors declare no conflict of interest.

## References

1. Wu F, Huo Y, Gao J. Coal mine gas emission prediction method based on forest regression. *Industry and Mine Automation* 2021; 47(8): 102–106. doi: 10.13272/j.issn.1671-251x.2021010024.
2. Zhang X, Liu F, Li X. Coal mine gas concentration prediction based on wavelet denoising and recurrent neural network. *Coal Technology* 2020; 39(9): 145–148. doi: 10.13301/j.cnki.ct.2020.09.041.
3. Zheng X, Lai W, Zhang L, Xue S. Quantitative evaluation of the indexes contribution to coal and gas outburst prediction based on machine learning. *Fuel* 2023; 338: 127389. doi: 10.1016/j.fuel.2023.127389.
4. Ji P, Shi S. Hazard prediction of coal and gas outburst based on the hamming distance artificial intelligence algorithm (HDAIA). *Journal of Safety Science and Resilience* 2023; 4: 151–158. doi: 10.1016/j.jnlssr.2022.12.001.
5. Xue F, Li X, Xu E. Application of GA-SVM coupling model in prediction coal and gas outburst. *Mineral Engineering Research* 2022; 37(3): 40–44. doi: 10.13582/j.cnki.1674-5876.2022.03.007.
6. Ji P, Shi S, Lu Y, Li H. Research on risk identification of coal and gas outburst based on PSO-CSA. *Mathematical Problem in Engineering* 2023; 2023: e5299986. doi: 10.1155/2023/5299986.
7. Lin H, Zhou J, Jin H, *et al.* Cooperative prediction method of coal and gas outburst risk grade based on feature selection and machine learning algorithm. *Journal of Mining & Safety Engineering* 2023; 40(2): 361–370. doi: 10.13545/j.cnki.jmse.2022.0010.
8. Fu H, Zhao J, Liu H, *et al.* Signal identification of fracture in gas bearing coal based on dual strategy coupling optimization. *China Safety Science Journal* 2022; 32(10): 40–47. doi: 10.16265/j.cnki.issn1003-3033.2022.10.1868.
9. Li B. Research on early warning method of coal and gas outburst based on deep learning and multi-source information fusion [PhD thesis]. Beijing: China University of Mining and Technology; 2021.

# Towards a solution to the problem of safety management of structurally complex systems

Alexander V. Bochkov

Scientific Secretary of Scientific and Technical Council, JSC NIIAS, Moscow 109029, Russia. E-mail: a.bochkov@gmail.com

## ARTICLE INFO

Received: 13 March 2023  
Accepted: 18 April 2023  
Available online: 5 May 2023

<http://dx.doi.org/10.59400/jam.v1i1.68>

Copyright © 2023 Author(s).

Journal of AppliedMath is published by Academic Publishing Pte. Ltd. This article is licensed under the Creative Commons Attribution-NonCommercial 4.0 International License (CC BY-NC 4.0). <https://creativecommons.org/licenses/by-nc/4.0/>

**ABSTRACT:** The non-isolation of modern, structurally complex, multi-purpose systems implies not only their interaction with the external environment, but also the impact of this environment on the systems themselves. The ability to predict and assess the consequences of these impacts, which are characterised by great uncertainty about the time, place and method of implementation, as well as the choice of a particular object of influence, is a task of extreme urgency in today's globalised world. If the stability of functioning of any structurally complex system is understood as the achievement by it of the purpose of its functioning with acceptable deviations on the volumes and times of implementation of private tasks, the safety management in this system is reduced, in fact, to minimisation of unplanned losses at the occurrence of abnormal situations of various kinds and to carrying out of measures for their prevention. The success of such tactics depends largely on the effectiveness of the risk management system, on the ability of decision-makers to foresee the possibility of poorly formalised threats turning into significant risks, i.e., on having methods and tools for ranking threats and significant risk factors. Inevitably, there is the task of setting protection priorities, ranking objectives (usually of different types), problems and threats, and reallocating available (usually limited) resources. The article considers the issues involved in building an integral security model that takes into account the risks to the assets being protected.

**KEYWORDS:** structurally complex system; objects of protection; security threat; risk; system significance; integral assessment

## 1. Introduction

Ensuring the security of any object implies a certain set of measures to counter threats to that object, i.e., the concept of threat is fundamental because the security system is based on it. The resolution of the uncertainty associated with the implementation of threats is achieved by building a security system based on the so-called principle of equal protection. This principle underlies, for example, the development of requirements to ensure the security of critical transport

infrastructure. The concepts considered in connection with the definition of threats allow to build the basic scheme of their interaction in the form of a model of threats to a separate object, group or class of homogeneous objects. For example, compressor stations of gas transportation systems can be recognised as homogeneous objects with respect to the spectrum of threats to critical elements of their infrastructure, since all types of these objects have the same infrastructure according to the intrasectoral classification and differ from each other only by the scale of

production activities and the characteristics of individual critical elements.

Both domestic and foreign researchers have paid attention to the problems of safety and stability studies of structurally complex technical systems. The reliability of technical systems and methods of their risk assessment were developed by Kumamoto and Henley<sup>[1]</sup>. Vemuri<sup>[2]</sup> considered typical characteristics of complex technical systems widely spread in the national economy, indicators of their efficiency, reliability, quality of management. In his works a lot of attention was paid to methods of modelling the most important classes of complex systems (mass service systems, discrete and continuous production processes). Interesting are the later studies of Rainshke and Ushakov<sup>[3,4]</sup>, in which they applied traditional models and approaches of reliability theory to solve problems of rational allocation of resources for protection of critical infrastructure objects. The logical and probabilistic approach to the analysis of reliability and safety of structurally complex systems was developed by Ryabinin<sup>[5]</sup>, Solozhentsev<sup>[6]</sup>, and Mozhaev *et al.*<sup>[7]</sup>. Glushkov *et al.*<sup>[8]</sup> introduced a new class of dynamical models based on nonlinear integro-differential equations with prehistory. They developed approaches to modelling so-called evolving systems, proved theorems on the existence and uniqueness of solutions describing their systems of equations.

In their papers, Ushakov<sup>[9-11]</sup> and Levitin<sup>[12]</sup> presented innovative approaches to the problem of protecting large numbers of critical facilities.

The work of these and many other authors has allowed us to view safety as a control problem. Since in most cases, the causes of an abnormal situation are combined; only part of the uncertainty that can be explained separately by external or separately by internal causes can be statistically eliminated. This problem can be solved by applying principles known from simulation and similarity theory.

Risk analysis is the only way to investigate those safety issues that cannot be answered by

statistics, such as accidents with low probability of occurrence but high potential consequences. Of course, risk analysis is not the solution to all safety problems, but it is the only way to compare risks from different hazards, highlight the most important ones, choose the most efficient and cost-effective systems to improve safety, develop measures to reduce the consequences of accidents, etc. It is important to remember that risk analysis issues cannot be considered separately from game formulation. Today, however, the main formulas used in risk analysis have been greatly simplified and their affiliation to game theory has almost been forgotten. Risk, as a dynamic property depending on time, means and information, has been reduced to “two-dimensional estimates” of probability and damage. It is possible to say that in modern risk analysis the theories of durability and reliability are “left”, but research on the theory of survivability, the theory of homeostasis, adaptive theories, including the theory of choice of decisions, the theory of perspective activity, the theory of reflexes, the theory of self-organising systems and others is curtailed.

## **2. General formulation of the safety management problem**

The non-isolation of a complex system implies its interaction with the external environment and the impact of that environment on it. This impact can be interpreted in a very broad sense: it can be natural disasters (e.g., earthquakes leading to the destruction of dams and other structures), large-scale accidents (e.g., an explosion in a nuclear power plant leading to the disruption of electricity supply to the entire region), as well as illegal actions, where the range of impact is the widest. Such malicious external influences are characterised by great uncertainty about the time, place and method of execution, as well as the choice of a specific object for the action.

The importance of the object to the initiator of such an “active action” coincides with the importance of that object to the owner of the system. More important objects require a higher level of protection because actions against them lead to more serious losses. It follows that the assessment of the systemic importance of the objects of a complex open-ended dynamic system should be carried out using the mathematical apparatus of game theory and, more generally, the theory of conflicting systems.

The first work formulating the principles of scientific analysis of actions in conflict situations, a book by Morgenstern and von Neumann<sup>[13]</sup>, was published in 1944. It unleashed a flood of mathematical research on games and solutions, which contributed significantly to the development of rules of optimal behaviour for a wide class of conflict situations, i.e., the development of optimal management strategies. Game theory, as it has developed to the present day, is inevitably normative in nature: the player applying it learns what he must do, what strategy he must choose, in order to secure a favourable outcome. But like many abstract mathematical models, the game-theoretic model of conflict is limited<sup>[14]</sup>. It cannot reveal the nature of conflict, the hidden sources of human activity in a conflict situation.

It is possible to put oneself in the position of one of the parties and to seek actions aimed at achieving a certain goal. In doing so, we must take into account the opposition of the opponent, whose goal is the opposite of ours. If, in this situation, we choose one of the possible strategies of behaviour, it is necessary to have a justification that this strategy is the best. We encounter this type of scheme when solving problems in operations research<sup>[15]</sup>. Since we rarely have all the necessary information about the “opponent” (about his goals, resources and strategies), we have to make decisions under conditions characterised by this or that degree of uncertainty, i.e., by the degree of ignorance of the party making the decision (i.e., the decision-maker (DM))

about these conditions. According to the information available about the “enemy” in the study of operations, the choice of strategy is usually based on the principle of a guaranteed result: whatever decision the “enemy” makes, the “defending” party must be guaranteed some gain. The conflict situation, although included in the model of an operation planned by one of the parties, is not the subject of independent research. In the specific tasks of operations research, the activity of the conflicting parties is not considered as a special type of human activity, and the conflict as such serves only as a background against which the actions of the parties are projected.

In mathematical game theory, the problem is much the same. Whether it is a real opponent or nature, the object of study is the choice of strategy, the choice of behaviour. The principle of a guaranteed outcome in game theory is concretised in the criteria for choosing a solution. The difference may be that “game theorists” work with game models from the position of objective research (both sides act in the model as equal partners), while researchers of operations necessarily take the position of one of the sides.

### **3. Model of the impact of on objects**

We can assume that the importance of the object to the system and to the intruder is in most cases the same, which means that the required level of object protection must be determined by considering the nature of possible attacks. Three sources, or combinations thereof, can be considered as such attacks.

Firstly, the most common “local crime” and related offences that affect the economic activity of facilities is usually theft. It also includes hooliganism (vandalism) and protest actions. The level of such crime is likely to correlate with the level of general crime in the region where the facility is located. The latent (hidden) part of this type of crime can be measured quite adequately by indicators such as the unemployment rate, the

proportion of migrants and the educational level of the population.

Second, there is the migration of domestic criminal and terrorist activity. Zones of active terrorist activity tend to grow: along with the migration of able-bodied people from “hot spots”, criminal groups “squeezed out” by law enforcement also migrate. The most telling indicator of this profile is the distance of the facility from areas of increased terrorist activity.

Third, these are specially trained terrorist and subversive groups, sent in whole or in part in the form of instructors from abroad. The actions they carry out are characterized by well-thought-out, preparedness and non-randomness (the planned nature of the activity and the weighted measurement of the feasibility of one or another action to inflict damage).

To solve the problem, the following approach is proposed by Bochkov<sup>[16,17]</sup>. Violators are classified according to their level of preparedness  $j$  ( $j = 0, 1, \dots, J$ ). Zero level ( $j = 0$ ) corresponds to the lowest level of preparedness. A maximum level ( $j = J$ ) corresponds to a super-prepared subversive group. Let us assume that an attack by an attacker of  $j$ -th level will require  $Z_j$  units of resources. It is natural to assume that the higher level  $j$  is, the more resources are needed  $Z_j$  (a more serious attack requires from intruders fundamentally more resources for its preparation: time, qualified personnel, studying functioning of objects and their security systems, etc.). It is also natural to suppose that the total resources of criminal world are limited (fighters, equipment, weapons), and hence the model of integral profile of intruders will be a tuple of number (intensity) of attacks of appropriate level of preparedness  $\vec{N} = \{N_0, N_1, \dots, N_J\}$  taking into account the above-mentioned limitations:

$$\begin{cases} N_j \leq N_{j,\max} \quad (j = 0, 1, \dots, J), \\ \sum_{j=0}^J (N_j \times Z_j) \leq Z, \end{cases} \quad (1)$$

where  $Z$  is the total amount of money allocated by crime to prepare and execute attacks on facilities.

The system of restrictions Equation (1) allows us in the problem under discussion to discard “extreme” variants, namely: the conditions of a terrorist or subversive “war”, when the value  $Z$  is large, as well as the conditions of a mass upsurge of low-preparedness crime (large  $N_{0,\max}$ , i.e., in other words, the system under study is not like a supermarket in terms of consumer value, so that the population rushes to “disperse valuables” available at its facilities). Dangerous industrial facilities, due to their fire and explosion hazard, are also remote enough from populated areas that they could be affected by a surge of vandalism.

Thus, in solving the problem of determining the systemic importance of targets, the criminal underworld is seen as a source of a variety of external attacks on targets, but a source that still has limited resources. High and medium level attacks pose the greatest threat. It is reasonable to assume that the criminal underworld will use the full range of its capabilities, i.e., we should expect both major attacks, which would “economically bankrupt” the owner, forcing him to spend excessive resources on reinforcing the physical protection of his facilities, and medium-prepared attacks, since over-prepared attacks are not feasible if the owner does not have the resources to protect all his facilities. For example, the level of protection of nuclear facilities for a system consisting of thousands of facilities is, in principle, unattainable.

In addition, crime is an active player: the choice of a target for an attack and a suitable way of carrying it out is an inherent advantage. At the same time, crime has an incomplete and inaccurate understanding of the current state of protection of the targets to be attacked, as well as the amount of damage it will cause if the attack is successful. These two nuances will be taken into account in further reasoning when formulating

an optimisation problem that matches the attacker model with the target model.

#### 4. Protection profile model

So, consider some ( $k$ -th) object. As a result of the supposed attack of intruders of this or that level of preparation to this object, through its complete (or partial) loss of serviceability, a certain damage will be caused. Let us denote it by  $X$ . Given that not every attack a priori leads to the success of the attacker, the protection profile of the  $k$ -th object can be described by interval representations by setting four matrices:

$$Q_{\min}^{[k]}(i, j), Q_{\max}^{[k]}(i, j), X_{\min}^{[k]}(i, j), X_{\max}^{[k]}(i, j) \quad (2)$$

where  $i$  ( $i = 0, 1, \dots, I^{[k]}$ ) level of protection of the  $k$ -th object (the zero level ( $i = 0$ ) corresponds to the current state of protection).

The interpretation of the matrix elements is as follows: if the specified object  $k$  with defense level  $i$  will be attacked by an adversary with preparedness level  $j$ , then with probability from  $Q_{\min}^{[k]}(i, j)$  to  $Q_{\max}^{[k]}(i, j)$  the whole system will be damaged with probability from  $X_{\min}^{[k]}(i, j)$  to  $X_{\max}^{[k]}(i, j)$ .

Clearly, the values of Equation (2) will increase as the level of preparedness of the “attacker”  $j$  increases and will decrease as the level of defense of the object  $i$  increases.

It is obvious that protection at any level requires certain material costs both on the part of the owner and the state. Let’s denote the cost of creating and maintaining object protection  $k$  at the  $i$ -th level as  $Y^{[k]}(i^{[k]})$ .

Since the total resource allocated to protect all objects is limited, the inequality must be satisfied:

$$\sum_k Y^{[k]}(i^{[k]}) \leq Y \quad (3)$$

where  $Y$  is the sum of all costs for the protection of objects under the assumption that for each object  $k$  the variant of protection system is chosen  $i^{[k]}$ .

If criminals did not have the advantage of target selection and attack options, that is, if criminality were indiscriminate like nature or technological failures, then the “optimal” security profile of objects could be achieved through the sequential execution of the following algorithm:

**Step 1.** Estimate the probabilities  $\lambda^{[k]}(j)$  of each  $k$ -th object being attacked by an adversary of  $j$ -th level of preparedness;

**Step 2.** Calculate the median value of the risk of an enemy attack on the  $k$ -th object  $j$  of level of readiness for the  $i^{[k]}$ -th variant of realization of the defense system of the object:

$$R[k; i^{[k]}] = \sum_{j=0}^J \left\{ \lambda^{[k]}(j) \times \left( \frac{Q_{\min}^{[k]}(i^{[k]}, j) + Q_{\max}^{[k]}(i^{[k]}, j)}{2} \right) \times \left( \frac{X_{\min}^{[k]}(i^{[k]}, j) + X_{\max}^{[k]}(i^{[k]}, j)}{2} \right) \right\} \quad (4)$$

**Step 3.** Determine the amount of risk averted per unit of funds invested in protection  $\theta[k, i^{[k]}]$ :

$$\theta[k, i^{[k]}] = \frac{R[k, i^{[k]}]}{Y^{[k]}(i^{[k]})} \quad (5)$$

**Step 4.** Select for each  $k$ -th object the maximum of the values  $\theta[k, i^{[k]}]$ :

$$\theta[k, i^{*[k]}] = \max_{i^{[k]}} \{ \theta[k, i^{[k]}] \} \quad (6)$$

i.e., at the chosen variant  $i^{*[k]}$  the maximum risk reduction per unit of invested funds for the  $k$ -th object is observed.

**Step 5.** Make a ranked list of objects, placing them in descending order of the value of the indicator  $\theta[k, i^{*[k]}]$  and then count the first  $\tilde{K}$  objects in the list such that the total cost of their protection is invested in the allocated funds

Y and for the  $(\tilde{K} + 1)$ -th object the resources are not enough.

The essence of the above procedure is simple and straightforward: it makes no sense to seek funds for additional protection for those objects that are not threatened by anything (the threat values of attacks are small  $\lambda^{[k]}(j)$ ). It is inexpedient to additionally protect those objects whose temporary loss of functionality has almost no effect on the value of total losses (i.e., small  $X_{\max}^{[k]}(i^{[k]}, j)$ ). And finally, additional protection is unreasonable for those objects that are already so well protected that the reduction of losses can be achieved in principle, but by inadequately large means (i.e., small values  $\theta[k, i^{*[k]}]$ ).

The key point of the algorithm described above is the compilation of a ranked list of objects by the criterion of minimizing the mathematical expectation of loss per unit of investment in their protection (in their sustainable functioning).

The Equation (4) clearly shows the need to collect and estimate data on three components: on the values of losses caused by the implementation of attacks  $X_{\min}^{[k]}(i, j)$ ,  $X_{\max}^{[k]}(i, j)$  and the indicator of “aggressiveness of criminal environment”  $\lambda^{[k]}(j)$  and on the dependence of risks on types of objects  $k$ .

The values of losses  $X$ , due to the fact that the objects of a complex system are not autonomous, should reflect the system effect (or socio-economic multi-effect), which increases significantly depending on which of the consumers of the products of the attacked object will suffer due to the reduction of its performance. Consequently, it is necessary to consider not the average, but the upper limits of damage indicators and to introduce an additional fourth component—the indicator of the importance of continuous operation of the object in connection with the cascade effect of strengthening the consequences of the object performance loss for other

objects of the system and other objects of other systems interacting with it.

Finally, the model additionally requires the introduction of another component, the need for which is due to the fact that the adversary implements an active, targeted choice of attack, while having value factors and priorities unknown either to security experts or to the competent authorities of the state, which shift values  $\lambda^{[k]}(j)$  from the “weighted average” (e.g., by industry). Sometimes, these “additional” values are specific: terrorists, for example, are prone to excessive bloodshed and hostage-taking, ritual murder, etc. Often, the systemic importance of protection of specific facilities temporarily increases during the stay there of the first persons of the state, ministers, especially during the commissioning of politically important production facilities not only internationally, but also regionally within the country. These circumstances should be taken into account and an additional component, the correction factor, should help.  $\mu^{[k]}$ , initially equal for all objects to unit, and which can be, according to LDP or experts, increased so that to increase the priority of inclusion of  $k$ -th object in the list of objects, equipped with additional protection measures for the reasons, not considered by rules, common for all objects. To some extent, the expediency of introducing the indicator  $\mu^{[k]}$ , becomes clearer from the following composition of the two models considered above.

## 5. Integration model

So let  $\tilde{Z}$  an estimate of the total resource available to the forces interested in violating the security of some objects. If  $\tilde{Z} < Z$ , then the defending party underestimates the adversary’s capabilities; if  $\tilde{Z} > Z$ , on the contrary, there is an overestimation of his forces. Further we will assume that at the moment of choosing the attack, the intruder has his own ideas about the amount of resources allocated by the owner to protect his objects, i.e., he also has some ideas about how

the “zero option” known to him could have changed.

Intruders have the right to choose targets, and they are able to choose the sets of objects they will attack. Let their choice be based on their own model of expected damage, that is, they have four analogous Equation (2) matrices at their disposal for each of the objects:  $\tilde{Q}_{\min}^{[k]}(i, j)$ ,  $\tilde{Q}_{\max}^{[k]}(i, j)$ ,  $\tilde{X}_{\min}^{[k]}(i, j)$ ,  $\tilde{X}_{\max}^{[k]}(i, j)$  and their own idea of how many resources  $\tilde{Y}$  is spent by the owner to protect all objects in the system. Similarly, if  $\tilde{Y} < Y$ , then the adversary underestimates the ability to protect the objects and, if  $\tilde{Y} > Y$ , then he overestimates them.

Obviously, the estimates  $\tilde{Q}_{\min}^{[k]}(i, j)$ ,  $\tilde{Q}_{\max}^{[k]}(i, j)$ ,  $\tilde{X}_{\min}^{[k]}(i, j)$ ,  $\tilde{X}_{\max}^{[k]}(i, j)$  can also be both overestimated and underestimated by intruders; nevertheless, in accordance with their right of choice, they choose such a set of objects for attack and such options of intruder preparedness for each object, at which the maximum damage is caused.

Let us denote the characteristic function by  $\delta^{[k]}(i, j)$ , which means that against the  $k$ -th object with the expected level of protection  $i$  ( $i = 0, 1, \dots, I^{[k]}$ ), the attack of level  $j$  ( $j = 0, 1, \dots, J^{[k]}$ ) is chosen. If for all  $i$  ( $i = 0, 1, \dots, I^{[k]}$ ), values of  $\delta^{[k]}(i, j)$  are equal to zero, then the  $k$ -th object will not be subject to an attack level of  $j$ . If for all  $j$  and all  $I$ , values of  $\delta^{[k]}(i, j)$  are equal to zero, then the  $k$ -th object under the enemy’s assumed targeting variant is completely dropped from the target list.

If for some  $\tilde{i}$ , value  $\delta^{[k]}(\tilde{i}, j(\tilde{i})) = 1$ , we consider that the object  $k$  with defense level 0 is chosen by the adversary as a target for an attack with the preparedness level  $j(\tilde{i})$ .

The listed properties are written down by a system of equations:

$$\begin{cases} \forall k \forall i \forall j \delta^{[k]}(i, j) \times (1 - \delta^{[k]}(i, j)) = 0, \\ \forall k \left( \sum_{i=0}^{I_k} \sum_{j=0}^J \delta^{[k]}(i, j) - 1 \right) \times \left( \sum_{i=0}^{I_k} \sum_{j=0}^J \delta^{[k]}(i, j) \right) = 0 \end{cases} \quad (7)$$

Considering that

$$\forall j \sum_{i=0}^{I_k} \sum_k \delta^{[k]}(i, j) = N_j \quad (8)$$

and supplementing Equations (7) and (8) with a system of constraints in Equation (1), then we obtain an estimate of the total damage to the object:

$$\begin{aligned} \tilde{R} &= \sum_k \sum_{i=0}^{I_k} \sum_{j=0}^J \left\{ \delta^{[k]}(i, j) \right. \\ &\times \left( \frac{Q_{\min}^{[k]}(i^{[k]}, j) + Q_{\max}^{[k]}(i^{[k]}, j)}{2} \right) \\ &\times \left. \left( \frac{X_{\min}^{[k]}(i^{[k]}, j) + X_{\max}^{[k]}(i^{[k]}, j)}{2} \right) \right\} \end{aligned} \quad (9)$$

Let us denote  $\tilde{R}$  as  $\tilde{R}(Var_I, Var_J)$ , underlining that  $\tilde{R}$  depends on both the variant of defending objects  $Var_I$ , and on the variant of the attack  $Var_J$ .

Looking for the maximum  $\tilde{R}$  for all variants of attacks satisfying the constraints, when considering all variants of equipping with additional protection as parameters:

$$\tilde{R}^*(Var_I) = \max_{Var_J} \{ \tilde{R}(Var_I, Var_J) \} \quad (10)$$

Thus, it is postulated that the adversary chooses the worst option for the defending party. Consequently, the problem of defense comes down to limiting the set of choices for the adversary—we look for such a reinforcement of objects that minimizes  $\tilde{R}^*(Var_I)$ . That is, the security management problem is reduced to find an equilibrium value  $\tilde{R}^{**}$ :

$$\tilde{R}^{**} = \min_{Var_I} \{ \tilde{R}^*(Var_I) \} \quad (11)$$

The proposed formulation has the typical form of game theory problems. The solution of this problem is a Nash equilibrium—saddle point  $(Var_{I^*}, Var_{J^*})$ :

$$\tilde{R}^{**} = \tilde{R}(Var_{I^*}, Var_{J^*}) \tag{12}$$

At this point, it is not advantageous for the defender to change his equipment strategy  $Var_{I^*}$ , because outside of this strategy, the opponent has opportunities for more “sensitive” strikes.

At the same time, it is not advantageous for the attacker to change his plan  $Var_{J^*}(Var_{I^*})$ , because any change leads to a reduction in the total damage it seeks to inflict on the individual objects of the system, and through them the entire system and the state as a whole.

The problem in this formulation theoretically has a very large dimension, has great combinatorial complexity, but is quite solvable due to the monotonicity of the criteria used and the linearity of the constraint systems.

The main problems in solving this problem are of an information-technological rather than a mathematical nature:

- For each  $k$ -th object, it is necessary to have estimates of the consequences of possible enemy attacks of different levels of preparedness  $j$ , which is not yet achievable in practice;
- For the whole system, it requires consideration of the risks to which objects are exposed, in a set of possible, including poorly formalized threats: the more effective optimization of protection is the more accurate the assessment of the potential capabilities of the enemy (and they are heterogeneous in both the technological and the regional aspect).

Within the framework of the considered statement, which takes into account the complex impact of a potential adversary, radically changes the understanding of assessing the effectiveness of defense systems. Thus, due to the limited resources available to intruders, it is natural to expect them to shift their targeting from well-

protected objects (with low expected effectiveness of attacks) to less protected objects (with greater effectiveness, but with less one-time damage).

Obviously, it is irrational to additionally protect facilities that are not attacked. Perhaps that is why they are not attacked, because routine work is being done to reinforce the guards. Another key element of the problem under consideration is that the search for effective solutions on both opposing sides lies largely in the information plane:

- The criminal, when preparing to attack a target, ideally looks for accomplices to help him choose a target that is achievable given his level of preparation and equipment;
- The defense system would have been capable of more concentrated counteraction if it had known the intentions of crime.

That is why in the description of the above-mentioned procedure, it has been repeatedly emphasised that we are talking only about assessments on both sides. Because of the irreducible uncertainty of the assessments, as a solution of the problem of working out the strategy and tactics of strengthening the protection of objects against possible illegal actions, including terrorist acts and attacks of subversive groups, it is reasonable to “load” the game statement<sup>[14]</sup>. In this coarsening, we should “idealise the enemy’s capabilities” and toughen the characteristics of possible losses, for example, by switching from median to maximum risk estimates.

As noted above, the adversary’s development of a plan begins with the procedure for selecting targets, i.e., their ranking. Since the meaning for the “attacker” and the “defender” is usually the same, let us consider the problem of ranking in more detail.

## 6. Model for assessing the level of impact of negative factors and justification of the scale of measurement of threats to the stability of the functioning of facilities, taking into account their specifics

Many current rating systems are based only on the results of the evaluation of one of the indicators describing the objects (for example, the activities of economic subjects, and their criticality)<sup>[19,20]</sup>.

However, in practice, both criticality and unconditional vulnerability of objects (in the problems of ranking objects by their system significance and ensuring safe functioning of these objects) are composed of a large number of assessments by private criteria. The importance of these criteria is not known in advance and the problem of multicriteria ranking<sup>[21,22]</sup> under conditions of uncertainty<sup>[23,24]</sup>. This is very important for the analysis of systems of with different purposes<sup>[25,26]</sup>.

### 6.1 Selection function language

Let us define on some set of objects  $O = \{o_1, \dots, o_D\}$  a logical function  $\pi: \pi(o) \rightarrow \{0,1\}$ , which indicates that the alternative  $o$  is mapped to some subset of  $\pi(o)$  ( $\pi(o) = 1$ ) or not ( $\pi(o) = 0$ ). The function  $\pi(o)$  will be called *the selection function*. The subset  $\pi(o)$ , in particular, can be a subset of the most systemically important critical infrastructure objects (CIPOs) or a subset of objects for which it is potentially necessary to implement additional protection measures. In general, the selection functions can be arbitrary, but in order for their use to give a correct description of the acts of selection, it is necessary to  $\pi(o)$  to impose a number of constraints or the so called axioms of choice<sup>[27]</sup>.

If the selection problem has a solution, it can be used to rank all objects  $O = \{o_1, \dots, o_D\}$  according to their systemic importance. Here  $D$  is the total number of objects.

With this in mind, let us describe the proposed ranking algorithm.

**Step 1.** By applying the function  $\pi(O)$ , we find the most systematically important objects  $\pi(O = O^{[1]+}) = O^{[1]} = \{o_{1,1}, \dots, o_{1,D_1}\}$ . Next, by “removing”  $D_1$  objects included in the  $O^{[1]}$  from  $O$ , we get an opportunity to make a choice on set of remained objects  $O^{[2]+} = O^{[1]+} \setminus O^{[1]}$ .

**Step 2.**  $D_2$  objects  $\pi(O^{[2]+}) = O^{[2]} = \{o_{2,1}, \dots, o_{2,D_2}\}$  followed by their deletion:  $O^{[3]+} = O^{[2]+} \setminus O^{[2]}$ .

Then, the procedure of selection and deletion at step  $s$  is repeated  $s = 3, 4, \dots$ :

$$\begin{cases} \pi(O^{[s]+}) = O^{[s]} = \{o_{s,1}, \dots, o_{s,D_s}\}, \\ O^{[s+1]+} = O^{[s]+} \setminus O^{[s]} \end{cases} \quad (13)$$

the algorithm is complete when all objects from the set  $O$  are “disassembled” into sets  $O^{[s]}$ :

$$\begin{cases} O = O^{[1]} \cup O^{[2]} \cup \dots \cup O^{[s]}, \\ D = D_1 + D_2 + \dots + D_s \end{cases} \quad (14)$$

The rule for determining the system significance of any object in this constructional solution is simple: the more significant the object is, the earlier  $s$  it is chosen as an element of the set  $O^{[s]}$ . The objects that happen to be in the same  $O^{[s]}$  are considered to be of equal importance.

But in the general case of the objects of a complex system perform different functions, different assessments of the results of their activities (or the consequences of their failure), and, therefore, it is important not only to know how much (how many times) one type of object is more significant than another, but also to be able to compare the estimates of objects of different types.

This requires the introduction of additional axioms specifying classes of selection functions among heterogeneous objects, but it should be understood that so far the general problem of selecting such axioms for collections of objects containing objects of different types has not been solved. There are several reasons for this, among the most important ones the following should be noted:

- large dimensionality of the choice problem;
- diversity of data;
- the presence of “missing values”;
- Noisiness: the presence of fuzzy and random indicators;
- multicriteria.

For these reasons, it is advisable to solve the problem of ranking a large set of objects of different types in several stages. At the first stage for objects of each type, it is necessary to construct private models of system significance estimation of objects of the selected type and to carry out the ranking by them. At the second stage, it is required to “stitch” the ranked lists of objects into a unified list. At the third stage, correction of values of estimations where it is necessary to take into account special conditions of functioning of separate objects is carried out.

To date, a number of standardized approaches to describing choice have been developed. The simplest option is to assume that for all alternatives  $x \in X$  can be given a function  $Q(x)$  which is called a criterion (a quality criterion, a target function, a preference function, a utility function, etc.) and has the property that if an alternative  $x_2$  is preferable to alternative  $x_1$ , then  $Q(x_2) > Q(x_1)$ . Choice as maximization of a criterion is reduced to the search for such a value  $x^* \in X$ , which achieves the maximum of function  $Q(x)$  on the set of alternatives  $X$ :  $x^* = \operatorname{argmax} Q(x)$ .

Often, however, constructing a utility function  $Q(x)$  is either very difficult or practically impossible, since the options being compared are similar to the choices for a person when he is offered either only “to drink” or only “to breathe”. At the same time, the ideas of construction of utility functions for choice can be useful at the initial stages of selection of variants when LDP on a limited amount of data tries to interpolate some nonlinear scale of utility.

## 6.2 On solving multi-criteria problems

The practice of decision-making in scientific, design, management and entrepreneurial activities shows that in the vast majority of cases there are several, and in some situations a very large number of criteria according to which it is necessary to optimise the parameters of technical systems or evaluate management decisions. Multi-criteria methods are used in problems where it is necessary to choose compromise solutions, for example between price and quality, expected profit and possible risk.

So, let the evaluation of an alternative  $x$  several criteria be used  $q_i(x)$  ( $i = 1, \dots, p$ ). If for  $x$ , there is an alternative  $x^*$ , which is not worse than  $x$  by all criteria  $q_i(x^*) \geq q_i(x)$  ( $i = 1, \dots, p$ ), and there is at least one criterion  $q_j(x)$  ( $j \in \{1, \dots, p\}$ ) such that a strict preference on this criterion is satisfied  $q_j(x^*) > q_j(x)$ , then we will say that  $x^*$  dominates over  $x$ , and the alternative  $x$  with respect to  $x^*$  is dominant. The relation between the elements of the set of alternatives introduced in this way defines a partial order relation on this set.

The variant  $x \in X$  will be called Pareto-optimal if there is no single option  $x^* \in X$  dominating  $x$ . The allocation of the set of Pareto-optimal solutions is the first step in the search for optimal alternatives. By construction, the elements of this set are incomparable with each other, and none of the Pareto-optimal solutions cannot be improved by any criterion without worsening the values of other criteria.

The Pareto-optimal set of solutions is constructed by discarding the dominant options. Initially, the Pareto-optimal set contains alternatives with maximum values of partial criteria. **Figure 1** illustrates the process of construction of such set in two-dimensional parameter space.

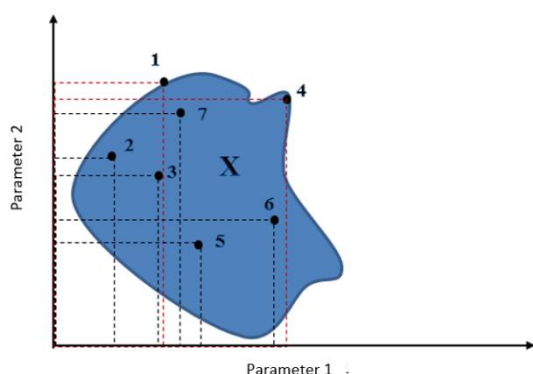


**Figure 1.** The process of building a Pareto-optimal set on many possible solutions.

For the solution variant, a rectangle is constructed, the corner points of which are the origin of coordinates and the point corresponding to the solution variant. **Figure 1** shows that point 1 dominates over points 2 and 3 (points 2 and 3 are inside the rectangle for point 1), and point 4 additionally dominates over points 5, 6, and 7. Thus, point 1 and point 4 form a Pareto-optimal set. The process is repeated for all points of the set  $X$ .

So, let the evaluation of an object  $o$  several criteria be used  $q_i(\vec{x}(o))$  ( $i = 1, \dots, r$ ). If for an object  $o$ , there is an alternative  $o^*$ , which is not worse than  $o$  according to all criteria  $q_i(\vec{x}(o^*)) \geq q_i(\vec{x}(o))$  ( $i = 1, \dots, r$ ), and there is at least one criterion  $q_j(\vec{x})$  ( $j \in \{1, \dots, r\}$ ) such that a strict preference on this criterion is satisfied  $q_j(\vec{x}(o^*)) > q_j(\vec{x}(o))$ , then we will say that  $o^*$  dominates over  $o$ . Accordingly, the alternative  $o$  with respect to  $o^*$  is dominant. As already mentioned, the relation between the elements of the set of alternatives introduced in this way defines a partial order relation on this set.

The variant  $o \in O$  will be called Pareto-optimal if there is no single option  $o^* \in O$  dominating  $o$ .

When the dimensionality is large  $r$ , it is likely that the set of Pareto-optimal solutions may consist not only of a large number of elements, but also have a complex multi-connected structure. Due to the fact that a limited number of objects and a limited number of coordinates in

which these objects admit a “visual” image are available to the LPR, there is a natural task of further selection of variants.

Note that when all criteria are a priori equivalent and it is impossible to replace some criteria by others, further selection (selection optimization) is impossible. In this case, the procedure of search for solutions of a multicriteria problem is completed by a list of Pareto-optimal solutions.

In other cases, the simplest variant of choosing the best variant is realized when the criteria are fundamentally unequal, namely, when the best variant is chosen from the previously selected candidates to the best ones. For this purpose, the so-called lexicographic ordering of the set is often used  $O$ : first in  $O$ , the best elements (variants of solutions) with the maximal value according to the criterion  $q_1$  and all other elements  $O$  are discarded. If the remaining subset contains more than one element, then the best elements by criterion are chosen among these elements  $q_2$ . Further, if necessary, it is necessary to optimize and discard options, using the criteria  $q_i$  ( $i = 3, \dots, r$ ) and so on, until there is only one element in the set  $O$ , it will be the desired solution.

In addition to lexicographic ordering, which gets its name from the arrangement of words in the dictionary and which almost immediately establishes a strict order on the set of objects under study, there are a number of constructive methods for solving problems of multicriteria choice due to the fact that a certain interchangeability of some criteria with others is allowed.

Consider, for example, the linear substitution method.

As in the method of lexicographic ordering, let the criteria  $q_i$  ( $i = 1, \dots, r$ ) be ordered in descending order of importance. Let us introduce replacement coefficients for the  $i$ -th criterion by the next  $(i+1)$ -th criterion in importance  $k_{i+1,i}$  ( $\forall i k_{i+1,i} > 1$  ( $i = 1, \dots, r - 1$ )). Thus we take into account that “loss” of a unit of criterion

$q_i$  can be “compensated” in principle by increasing of criterion  $q_{i+1}$ , but only if compensation is done “with percents” (Figure 2).

So the option  $o_2$  turns out to be preferable than  $o_1$ , because the loss of  $q_1(o_1) - q_1(o_2)$  units by the first criterion is “more than compensated” by the gain by the second criterion  $q_2(o_2) - q_2(o_1)$ .

If concessions of any size are admissible, the method is reduced to a non-strict ordering of Pareto-optimal solutions with the help of the generalized criterion  $q_0(x)$  as a weighted linear convolution of private criteria:

$$q_0(x) = 1 \times q_1(x) + (k_{2,1})^{-1} \times q_2(x) + (k_{3,2} \cdot k_{2,1})^{-1} \times q_3(x) + \dots + (k_{p,p-1} \cdot \dots \cdot k_{2,1})^{-1} \times q_r(x) \tag{15}$$

If the size of the concessions is limited, then locally the optimal option is quickly found, because the options that require large size concessions are not considered. The method with limited concessions is reasonable to use in cases where the set of possible options  $O$  can be replenished.

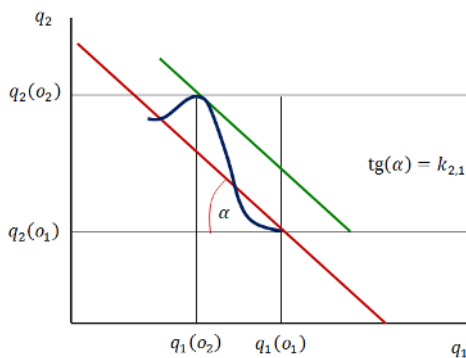


Figure 2. Illustration of the linear substitution method.

It should be noted that optimization using additive linear criterion  $q_0(x)$  leads to solutions on the boundaries of the admissible domain  $O$  which relates the problem of finding the optimal choice of an option to linear programming problems.

When the values of particular criteria  $q_i$  ( $i = 2, \dots, r$ ) are considered as coefficients

that strengthen (weaken) the system significance estimated through the previously constructed criteria, the equation for the general criterion of “hyperbolic” substitution will take the following form:

$$\log(q_0(x)) = 1 \times \log(q_1(x)) + (\tilde{k}_{2,1})^{-1} \times \log(q_2(x)) + (\tilde{k}_{3,2} \cdot \tilde{k}_{2,1})^{-1} \times \log(q_3(x)) + \dots + (\tilde{k}_{p,p-1} \cdot \dots \cdot \tilde{k}_{2,1})^{-1} \times \log(q_r(x)) \tag{16}$$

In Equation (16), the coefficients with tilde are the coefficients of linear substitution of criteria presented in logarithmic scales.

Potentiating Equation (15), we obtain another form of the generalized criterion:

$$q_0(x) = (q_1(x)) \times (q_2(x))^{(\tilde{k}_{2,1})^{-1}} \times (q_3(x))^{(\tilde{k}_{3,2} \cdot \tilde{k}_{2,1})^{-1}} \times \dots \times (q_r(x))^{(\tilde{k}_{p,p-1} \cdot \dots \cdot \tilde{k}_{2,1})^{-1}} \tag{17}$$

If private criteria are properly scaled during construction, the coefficients marked with “tilde” will become equal to one, and the index of system significance  $q_0(x)$  will be the product of basic index  $q_1(x)$  by the product of criteria-dimensionless “correction” coefficients. Their number  $(r - 1)$  is determined by how many will be needed to remove contradictions in the examples of the training sample, i.e., according to the scheme similar to the one presented in the previous section.

Note that, as a rule,  $q_0(q_1, \dots, q_p)$  is assumed to be a monotonically increasing bounded unit positive function of its arguments. Hence, every projection of a convolution function  $q_0(q_1, \dots, q_p)$  when some of its arguments take fixed values, there will also be a monotonic function of the remaining arguments. This al-

lows us to construct the convolution  $q_0$  or super-criterion as a monotone superposition of monotone superpositions, etc.

As such, monotonic convolution functions are used additive (Equation (18)) or multiplicative (Equation (19)) functions.

$$q_0(q_1, \dots, q_p) = \sum_{i=1}^3 \frac{\alpha_i}{S_i} \times q_i \tag{18}$$

$$q_0(q_1, \dots, q_p) = 1 - \prod_{i=1}^p \left(1 - \frac{\beta_i}{S_i} \times q_i\right) \tag{19}$$

Coefficients  $\alpha_i$  и  $\beta_i$  in Equation (18) and (19) reflect the weight coefficients of the criteria  $q_i$ . The coefficients  $s_i$  are chosen so as to make dimensionless the numbers  $q_i$  and, if needed, to provide their normalization  $0 \leq \left(\frac{\beta_i}{S_i} \times q_i\right) \leq 1$ . In practice, the parameters  $\alpha_i$  and  $\beta_i$  are determined by training on a finite set of examples.

A practical application of the risk synthesis concept described with a notional calculation example is given in other author’s work<sup>[28]</sup>.

## 7. Concluions

At present, it is more important than ever to develop theoretical foundations and to construct models and technological tools of information-analytical work in the field of decision support that are adequate to the existing challenges, with the aim of ensuring the complex security of structurally complex systems. Inevitably, there is a need to identify priorities, rank objectives, problems and threats, and reallocate available (usually limited) resources.

It is shown that the task of ranking critical objects by system importance leads to the problem of multicriteria ranking under uncertainty, which is of great importance for the analysis of structurally complex systems with different purposes. Since in the general case, the objects of a complex system perform different functions and the results of their activity (or the consequences

of their failure) are estimated differently, it is important not only to know how much (how often) one object of the same type is more important than another, but also to be able to compare the estimates of objects of different types. For this purpose, additional axioms are introduced that concretise the classes of functions of a choice among heterogeneous objects. A solution to the problem, of the Pareto analysis type, is proposed, which makes it possible to select the parts (objects) of the system under study that require priority attention from the point of view of their safety.

The presented algorithm provides decision support in the so-called problem of group selection of critical infrastructure objects of a structurally complex system that require increased attention in terms of their protection against the existing range of threats, taking into account the resources required for this. Such problems arise in the analysis and aggregation of heterogeneous information about the preferences of compared objects into a single “group” preference.

The algorithm is based on game theory with a set of assumptions about the resources of intruders attacking the system (negative action factors) and its “defenders”. The algorithm allows to reasonably align scales of system importance of objects of different types, i.e., to embed objects described by different resource and basic criteria in a single scale of comparison.

The obtained results can be applied in critical industries—complex process control systems, transport, aerospace and military spheres, banking and financial structures, as well as in central and sectoral management bodies for methodological and technical support of relevant decision-making.

## Conflict of interest

The author declares no conflict of interest.

## References

1. Henley EJ, Kumamoto X. Reliability of technical systems and risk assessment (Russian). Mashinostroenie; 1984.
2. Vemuri V. Modeling of complex systems. Academic Press; 1978.
3. Rainshke K, Ushakov IA. Evaluation of the reliability of systems using graphs (Russian). Radio and Communications; 1988. p. 208.
4. Ushakov IA. Counter-terrorism: Protection resources allocation. In: Reliability: Theory & applications. Wiley; 2006.
5. Ryabinin IA. Reliability and safety of structurally complex systems (Russian). St. Petersburg University Publisher; 2007.
6. Solozhentsev ED. Scenario logic and probabilistic management of risk in business and engineering. New York: Springer; 2004.
7. Mozhaev AS, Gladkova IA, Musaev AA. Method of logic-deterministic modeling of network systems (Russian). Izvestiya St. Petersburg State Technological Institute (Technical University) 2012; 14: 89–96.
8. Glushkov VM, Ivanov VV, Yanenko VM. Modeling of developing systems (Russian). Nauka; 1983. p. 351.
9. Ushakov I. Counter-terrorism: Protection resources allocation. Part I. Minimax criterion. Reliability: Theory and Applications 2006; 1(2).
10. Ushakov I. Counter-terrorism: Protection resources allocation. Part II. Branching system. Reliability: Theory and Applications 2006; 1(3).
11. Ushakov I. Counter-terrorism: Protection resources allocation. Part III. Fictional “case study”. Reliability: Theory and Applications 2007; 2(1).
12. Levitin G. Optimal defense strategy against intentional attacks. *IEEE Transactions on Reliability* 2007; 56(1): 148–157. doi: 10.1109/TR.2006.884599.
13. Mongerstern O, von Neumann J. Game theory and economic behavior (Russian). Nauka; 1970. p. 708.
14. Lefebvre VA, Smolyan GL. In: Tsygichko VN (editor). Algebra of conflict (Russian). 6<sup>th</sup> ed. LENAND; 2018. p. 72.
15. Smolyan GL. Operations research—An instrument of effective management (Russian). Znanie; 1967.
16. Bochkov AV. Hazard and risk assessment and mitigation for objects of critical infrastructure. In: Ram M, Davim JP (editors). Diagnostic techniques in industrial engineering. Management and industrial engineering. Springer Cham; 2017. p. 57–135.
17. Bochkov AV. Approaches to the construction of adaptive situation control systems of structurally complex systems under uncertainty. In: Proceedings of the International Conference ISAHP-2011; 15–18 June 2011; Sorrento, Naples, Italy.
18. Bochkov AV, Zhigirev NN, Lesnykh VV. Dynamic multi-criteria decision making method for sustainability risk analysis of structurally complex techno-economic systems. Reliability: Theory & Applications 2012; 1(25): 36–42.
19. Karminsky AM, Peresetsky AA, Petrov AE. Ratings in economics: Methodology and practice (Russian). Finance and Statistics; 2005.
20. Baranov S, Skufyina T. Analysis of inter-regional differentiation and the construction of rankings of the subjects of the Russian Federation (Russian). *Voprosy Ekonomiki* 2005; 8: 54–75. doi: 10.32609/0042-8736-2005-8-54-75.
21. Larichev OI. A property of decision-making methods in multi-criteria individual choice problems. *Automation and Remote Control* 2002; 63(2): 304–315. doi: 10.1023/A:1014207910716.
22. Keeney RL, Raiffa H. Decisions with multiple objectives: Preferences and value tradeoffs. Cambridge University Press; 1993. p. 569.
23. Kuvshinov BM, Shaposhnik II, Shiryaev VI, Shiryaev OV. Using committees in problems of pattern recognition with inaccurate expert estimates (Russian). *Izvestiya Chelyabinskogo Nauchnogo Center* 2001; 2(11): 81–88.
24. Mazurov VD. The Method of Committees in Problems of Optimization and Classification (Russian). Nauka; 1990.
25. Zhukovsky VI. Cooperative games under uncertainty and their applications (Russian). Editorial URSS; 1999.
26. Kweid E. Analysis of complex systems (Russian). Soviet Radio; 1969.
27. Podinovsky VV. Decision under multiple estimates for the importance coefficients of criteria and probabilities of values of uncertain factors in the aim function. *Automation and Remote Control* 2004; 65: 1817–1833. doi: 10.1023/B:AURC.0000047896.61645.43.

28. Bochkov A, Lesnykh V, Zhigirev N, Lavrukhin Y. Some methodical aspects of critical infrastructure protection. *Safety Science* 2015; 79: 229–242. doi: 10.1016/j.ssci.2015.06.008.

# Sustainable information into portfolio optimization models

Gabriele Sbaiz

Department of Economics, Business, Mathematics and Statistics, University of Trieste, 34127 Trieste, Italy. E-mail: gabriele.sbaiz@deams.units.it

## ARTICLE INFO

Received: 3 April 2023  
Accepted: 24 May 2023  
Available online: 28 May 2023

<http://dx.doi.org/10.59400/jam.v1i1.125>

Copyright © 2023 Author(s).

*Journal of AppliedMath* is published by Academic Publishing Pte. Ltd. This article is licensed under the Creative Commons Attribution-NonCommercial 4.0 International License (CC BY-NC 4.0).  
<https://creativecommons.org/licenses/by-nc/4.0/>

**ABSTRACT:** In the last fifteen years, extreme events such as the global financial and economic crisis of 2007–2008 and the Covid-19 pandemic have highlighted the importance of corporate social responsibility and sustainability in different aspects of our society. The environmental, social, and governance (ESG) disclosures have also gained increasing significance for investors due to initiatives undertaken by international bodies. In particular, with the Action Plan in 2018, the European Commission has assigned specific responsibilities to financial intermediaries to drive flows toward sustainable investments, explicitly requiring portfolio managers to integrate these non-financial factors into their decision-making processes. More and more, asset management firms and insurance companies offer tailored products to meet their customers' sustainable needs and desires. This trend implies a growing recognition of sustainable practices in the financial sector, emphasized by the need to integrate ESG considerations in investment strategies.

**KEYWORDS:** computational finance; sustainable portfolios; ESG ratings; investor's preferences; single- and multi-objective optimization

## A gentle introduction

The traditional mean-risk framework, which represents the modern portfolio theory's milestone, was first formulated by Markowitz<sup>[1]</sup> in the 1950s. In this frame, the investors are rational and risk-averse, meaning they seek to maximize their returns while minimizing risk simultaneously. However, this model, which focuses solely on financial features, is blind to the increasing sensitivity of political institutions, portfolio managers, and new generations of investors toward the planet's sustainable development. Thus, a new paradigm involving the impact of investment choices on the environment and society is needed.

Several methodologies have been proposed in the literature to incorporate ESG scores into the portfolio optimization process. In particular, this sustainable information has three main uses: the ESG criteria are employed as a discriminant in the preselection strategies; the ESG ratings are viewed

as a constraint of the optimization process; the ESG information is handled as an objective function in the optimization problem.

The first approach for responsible investments involves a preselection strategy based on the ESG information to exclude assets that are not sustainable and ethical enough. For example, Liagkouras *et al.*<sup>[2]</sup> have adopted a screening procedure to identify a subset of ESG-compliant stocks as constituents of a Mean-Variance (M-V) portfolio. Kaucic *et al.*<sup>[3]</sup> have studied several ESG-based preselection techniques in a prospect theory-based portfolio model.

In a second approach, the ESG scores are employed to define a constraint establishing the minimum acceptable sustainable grade of portfolios. Following this approach, De Spiegeleer *et al.*<sup>[4]</sup> have extended the M-V model. Afterward, Morelli<sup>[5]</sup>, exploiting only the environmental scores, has incorporated a constraint on the selected

parameter in the Mean-CVaR model.

Alternatively, instead of setting a minimum threshold for the portfolio ESG score, a third approach directly includes the sustainable information into the objective function of the optimization problem. Schmidt<sup>[6]</sup> has modified the single-objective function of the M-V model so that portfolio weights are simultaneously optimized in terms of return, risk, and ESG value. This formulation includes two parameters: the risk-aversion parameter, which controls the risk-return trade-off, and the so-called ESG-strength parameter, which reflects the investors' sustainable preferences. In the multi-objective optimization context, Garcia-Bernabeu *et al.*<sup>[7]</sup> have extended the classical bi-criteria M-V framework by directly including sustainability as a third criterion. They formalized the preference relation of an ESG-aware M-V investor and introduced a multi-objective evolutionary algorithm to solve the optimal allocation problem. In a similar way, Hilario-Caballero *et al.*<sup>[8]</sup> have employed a multi-objective approach to include the investor's preferences toward the portfolio's carbon risk exposure into the bi-criteria M-V optimization problem. Pedersen *et al.*<sup>[9]</sup> have constructed the ESG-efficient frontier, showing the highest attainable Sharpe ratio for each ESG level, and they have investigated the costs and benefits of responsible investing. Xidonas and Essner<sup>[10]</sup> have proposed a multi-objective minimax-based optimization model to build up optimal ESG portfolios that maximize the risk performance across the environmental, social and governance components of the ESG criteria. Cesarone *et al.*<sup>[11]</sup> have implemented the standard  $\epsilon$ -constrained method to solve the tri-objective M-V-ESG optimization problem. Finally, Lindquist *et al.*<sup>[12]</sup> have combined ESG scores with financial returns to generate an ESG-valued return and applied this measure in a general mean-risk optimization framework.

To sum up, the last twenty years have strengthened the importance of ESG in finance, not only from the stakeholder point of view but also from the shareholder perspective. As a consequence, some questions arise naturally:

- What is the impact of ESG investing on risk premia?
- What is the impact of ESG screening on portfolio returns?

## Conflict of interest

The author declares no conflict of interest.

## References

1. Markowitz H. Portfolio selection. *The Journal of Finance* 1952; 7(1): 77–91.
2. Liagkouras K, Metaxiotis K, Tsihrintzis G. Incorporating environmental and social considerations into the portfolio optimization process. *Annals of Operations Research* 2022; 316: 1493–1518. doi: 10.1007/s10479-020-03554-3.
3. Kaucic M, Piccotto F, Sbaiz G, Valentinuz G. Optimal portfolio with sustainable attitudes under cumulative prospect theory. *Journal of Applied Finance & Banking* 2023; 13(4): 65–86. doi: 10.47260/jafb/1344.
4. De Spiegeleer J, Höcht S, Jakubowski D, *et al.* ESG: A new dimension in portfolio allocation. *Journal of Sustainable Finance & Investment* 2023; 13(2): 827–867. doi: 10.1080/20430795.2021.1923336.
5. Morelli G. Responsible investing and portfolio selection: A shapley - CVaR approach. *Annals of Operations Research* 2023. doi: 10.1007/s10479-022-05144-x.
6. Schmidt AB. Optimal ESG portfolios: An example for the Dow Jones index. *Journal of Sustainable Finance & Investment* 2022; 12(2): 529–535. doi: 10.1080/20430795.2020.1783180.
7. Garcia-Bernabeu A, Salcedo JV, Hilario A, *et al.* Computing the mean-variance-sustainability non-dominated surface by Ev-MOGA. *Complexity* 2019; 2019: 6095712. doi: 10.1155/2019/6095712.
8. Hilario-Caballero A, Garcia-Bernabeu A, Salcedo JV, Vercher M. Tri-criterion model for constructing low-carbon mutual fund portfolios: A preference-based multi-objective genetic algorithm approach. *International Journal of Environmental Research and Public Health* 2020; 17(17): 6324. doi: 10.3390/ijerph17176324.
9. Pedersen LH, Fitzgibbons S, Pomorski L. Responsible investing: The ESG-efficient frontier. *Journal of Financial Economics* 2021; 142(2): 572–597. doi: 10.1016/j.jfineco.2020.11.001.

10. Xidonas P, Essner E. On ESG portfolio construction: A multi-objective optimization approach. *Computational Economics* 2022; doi: 10.1007/s10614-022-10327-6. Sustainability 2022; 14(4): 2050. doi: 10.3390/su14042050.
11. Cesarone F, Martino ML, Carleo A. Does ESG impact really enhance portfolio profitability? *Advanced REIT portfolio optimization: Innovative tools for risk management*. Springer; 2022.
12. Lindquist WB, Rachev ST, Hu Y, Shirvani A. *Advanced REIT portfolio optimization: Innovative tools for risk management*. Springer; 2022.

# Impact of Hindustani ragas in stress management: A statistical study

Soubhik Chakraborty<sup>1,\*</sup>, Avinav Prasad<sup>1</sup>, Apoorva Chakraborty<sup>2</sup>, Prerna Singh<sup>1</sup>

<sup>1</sup> Department of Mathematics, Birla Institute of Technology, Mesra, Ranchi 835215, India

<sup>2</sup> Sangeet Visharad and PG Diploma in Music Therapy, Former Student, NADA Centre for Music Therapy, New Delhi 110064, India

\* Corresponding author: Soubhik Chakraborty, soubhikc@yahoo.co.in

## ARTICLE INFO

Received: 26 April 2023  
Accepted: 26 May 2023  
Available online: 8 June 2023

<http://dx.doi.org/10.59400/jam.v1i1.143>

Copyright © 2023 Author(s).

Journal of AppliedMath is published by Academic Publishing Pte. Ltd. This article is licensed under the Creative Commons Attribution-NonCommercial 4.0 International License (CC BY-NC 4.0).  
<https://creativecommons.org/licenses/by-nc/4.0/>

**ABSTRACT:** This work is a part of our ongoing research project entitled *Hindustani Raga Analysis Using Statistical Musicology with Therapeutic Applications for Stress Management*. Using the perceived stress scale (PSS), baseline data were collected on 28 participants, 14 for the control group (non-music intervention group) and the remaining 14 for the case group (music intervention group), the allotment of a participant to one of the groups being done using randomized control trial (RCT) to prevent bias in allocation. After 5 music therapy sessions, the follow-up data were collected and the scores (0, 1, 2, 3, 4) were filled for the 10 questions in the questionnaire of the PSS scale. The rating is 0–13 implying low stress, 14–26 implying moderate stress and 27–40 implying high stress. As per the PSS rule, those having stress levels below 13 were dropped from the study. Thus, the actual number of participants in both groups would be less than those interviewed (sample size  $n = 7$  for each group). Using paired  $t$  test, it is found that the case group participants have shown considerable improvement in comparison to the control group. Thus, the efficacy of music intervention in combatting stress is established.

**KEYWORDS:** perceived stress scale; paired  $t$  test; music therapy; Hindustani raga; music transcriber

**AMS/ MSC CLASSIFICATION:** 62P99

## 1. Introduction

Scientists through their studies have revealed the healing powers of music in controlling blood pressure, negative emotions and stress. Statistics and probability have been used to analyze music successfully both in western and non-western (including Indian) music. For details, please refer to the books by Thaut<sup>[1]</sup>, Beran<sup>[2]</sup>, Temperley<sup>[3]</sup>, Tewari and Chakraborty<sup>[4]</sup> and Patel<sup>[5]</sup> and the references cited therein, while the paper by Singh *et al.*<sup>[6]</sup> provides a brief survey on music intervention in both western and non-western (Indian) music. In an earlier work, Priyadarshini and Chakraborty<sup>[7]</sup> used statistical

modeling, inter-onset interval and rate of change of pitch (pitch velocity) to distinguish between restful and restless ragas in Hindustani classical music. In Indian classical music (both Hindustani and Carnatic), a raga may be defined as a melodic structure with fixed notes and a set of rules that characterize a particular mood conveyed by performance<sup>[8]</sup>.

## 2. Literature review

Aldridge<sup>[9]</sup> provides a good source of literature review on music therapy. The main emphasis on music therapy intervention is on the soothing ability of music and the necessity of music as

an antidote to an overly technological medical approach. Most of these articles are concerned with receptive (passive) music therapy and the playing of pre-recorded music on patients emphasizing the need for healthy pleasures like music, fragrance and aesthetic visuals for the reduction of stress and the enhancement of well-being. The overall expectation is that the recreational, emotional and physical health of the patients would improve<sup>[10]</sup>. A good account of research findings about the neurobiological foundation of rhythm and the brain with a thrust on how music can affect both musical and non-musical brains can be found in Thaut<sup>[1]</sup> which gives the new therapeutic methodology of neurologic music therapy dealing extensively with clinical techniques and implementations in rehabilitation. Sarkamo and Soto<sup>[11]</sup> found that listening to pleasant music can have a facilitating effect on visual awareness in patients with visual neglect, which is associated with functional coupling between the emotional and attentional areas of the brain region. Secondly, daily music listening can improve auditory and verbal memory, focused attention, and mood as well as induce structural gray matter changes in the early post-stroke stage. Although some information on music therapy in the context of Indian music is available (Sairam<sup>[12]</sup>, Rammohan<sup>[13]</sup>, Singh et al.<sup>[14]</sup>), it is seriously limited. Scientific research in Indian music especially from a therapeutic angle is still at the beginning stage. Thus, there is a clear gap in music therapy research in western music and the Indian counterpart and this motivated us to experiment with Hindustani ragas to combat stress.

### 3. Our contribution

A project titled *Hindustani Raga Analysis Using Statistical Musicology with Therapeutic Applications for Stress Management* is currently underway in our institute in which the first author is officiating as a principal investigator, the second author is developing a music therapy app, the third author, a certified music therapist, is guiding the

music therapy interventions and the fourth author, who has joined this project as a project fellow, is working on a music transcriber.

The objective of the project, novelty and deliverables are outlined next.

- Objective: building a music transcriber and a music therapy app to combat stress by analyzing and applying the melodic structure of Hindustani ragas using statistical musicology. Statistics being the science of exploring and studying patterns in numerical data will be helpful in relating the musical patterns with the corresponding emotional changes in the brain. Musical data are numerical and hence allow statistical analysis.

- Novelty: building a music transcriber & music therapy app to control stress using Hindustani ragas. The transcriber will provide the musical data in digitized form using the STFT algorithm (Short-time Fourier transform). The musical data would provide information on note duration, inter-onset interval, pitch velocity & pitch movements between notes. The project fellow who has joined this project is working on it using MATLAB and Python coding. The working of the music therapy app is given in Section 6.

- Deliverables: music transcriber, music therapy app, and research papers/monograph on Hindustani ragas.

## 4. Methodology: Perceived stress scale (PSS); paired $t$ test

### 4.1. The perceived stress scale (PSS)

PSS is a classic stress assessment instrument.

The tool, while originally developed in 1983, remains a popular choice for helping us understand how different situations affect our feelings and our perceived stress. Refer to perceived stress scale<sup>[15]</sup> for further details on the questionnaire and scoring in PSS.

### 4.2. Paired $t$ test

Paired  $t$  test is always used on the same group of individuals. Thus, if  $x_i$  is the PSS score

at baseline and  $y_i$  is the PSS score after music therapy intervention for the  $i$ -th individual,  $i = 1, 2, \dots, n$  for  $n$  individuals, we calculate the statistic.

$t = d_{mean}/[sd/\{SQRT(n)\}]$  which follows student's  $t$  distribution with  $(n - 1)$  degrees of freedom (d.f.), where  $d_i = x_i - y_i$ ,  $d_{mean} = \Sigma d_i/n$  and  $sd^2 = [1/(n - 1)]\Sigma(d_i - d_{mean})^2$ , where the summation extends over  $i = 1$  to  $n$ .  $SQRT$  implies square root.

Here our null hypothesis is that the difference  $d_i$  values are due to sampling fluctuations only which would be rejected if the calculated value of  $t$  exceeds the tabulated  $t$  with  $n - 1$  degrees of freedom and 5% level of significance.

### 5. Summary of the experimental results

Using PSS (perceived stress scale) baseline data were collected on 28 participants, 14 for the control group (non-music intervention group) and the remaining 14 for the case group (music intervention group), the allotment of a participant to one of the groups being done using randomized control trial (RCT) to prevent bias in allocation. Each participant is identified by a unique (roll) number and is allocated to one of the two groups randomly with equal probability using RCT. After 5 music therapy sessions covered in 45 days, the follow-up data have been collected. The participants were personally interviewed by a certified music therapist and her assistant and scores (0, 1, 2, 3, 4) were filled for the 10 questions in the questionnaire of the PSS scale. The questions in the PSS scale are such that, for some questions, less score is desirable while for others, more score is better. To induce uniformity, the scores were reversed for the latter

type of questions so that after reversing, for all questions, less score is deemed as better. Now the scores from the 10 questions were added and this sum is our variable under study. The rating is 0–13 implying low stress, 14–26 implying moderate stress and 27–40 implying high stress. As per the PSS rule, those having stress levels below 13 were dropped from the study. Thus, the actual number of participants in both groups would be less than those interviewed (sample size  $n = 7$  for each group). Using paired  $t$  test, it is found that the case group participants have shown considerable improvement in comparison to the control group. Thus the efficacy of music intervention in combatting stress is established, since the allocation of the participants to both the groups was done by RCT.

Place of study (data collection): Department of Mathematics, Birla Institute of Technology, Mesra, Ranchi-835215, India.

Place of music therapy intervention: Music Room, Birla Institute of Technology, Mesra, Ranchi-835215, India.

Results of paired  $t$  test applied to the control group and the case group participants.

Let  $\mu_d = E(d) = E(X - Y)$  for the control group:

$H_0: \mu_d = 0$  (not undergoing music therapy does not have any effect on PSS score);

$H_1: \mu_d < 0$  (not undergoing music therapy worsens the PSS score);

$\alpha: 5\%$ .

Test statistic: paired  $t = d_{mean}/[sd/\{SQRT(n)\}] \sim t_{(n-1)d.f.}$

Solution:

The analysis of the PSS scores for the control group participants is shown in **Table 1**.

**Table 1.** Analysis of PSS score for control group participants

Participant No.	The control group		
$i$	Pre test PSS score ( $X_i$ )	Post test PSS score ( $Y_i$ )	$d_i = X_i - Y_i$
1	17	23	-6
2	26	32	-6
3	22	26	-4
4	17	21	-4
5	21	22	-1
6	24	28	-4
7	22	18	-4

$$d_{mean} = -29/7 = -4.142857$$

variance of

$$d = Var(d) = \Sigma d_i^2/n - (d_{mean})^2$$

$$= (36 + 36 + 16 + 16 + 1 + 16 + 16)/7 - (4.142857)^2$$

$$= 19.571429 - 17.163264$$

$$= 2.408165$$

$sd = +SQRT(2.408165) = 1.551826$   
 where  $+SQRT$  implies positive square root is to be taken.

$$t = (-4.142857)/(1.551826/2.645751)$$

$$= -7.063273$$

Table  $t_{0.05}$  for  $7 - 1 = 6$  d.f. for one tailed test = 1.94 (equivalent to table  $t$  at 10% level of significance for two tailed test as seen from  $t$  table).

As calculated  $t <$  table  $t$ , the null hypothesis is rejected and we conclude that the PSS score of

the control group not subjected to music therapy worsened possibly due to examination stress, job insecurity and other factors.

For the case group:

$H_0: \mu_d = 0$  (undergoing music therapy does not have any impact on the PSS score);

$H_1: \mu_d > 0$  (undergoing music therapy significantly lowers the PSS score; i.e., music therapy is able to combat stress);

$\alpha: 5\%$ .

Test statistic: paired  $t = d_{mean}/[sd/\{SQRT(n)\}]$

$\sim t_{(n-1)d.f.}$

Solution:

The analysis of the PSS scores for case group participants is shown in **Table 2**.

**Table 2.** Analysis of PSS score for case group participants

Participant No.	The case group		
$i$	Pre test PSS score ( $X_i$ )	Post test PSS score ( $Y_i$ )	$d_i = X_i - Y_i$
1	19	10	9
2	21	7	14
3	24	12	12
4	21	13	8
5	28	8	20
6	24	9	15
7	22	5	17

$$d_{mean} = 95/7 = 13.571429$$

variance of

$$d = Var(d) = \frac{\Sigma d_i^2}{n} - (d_{mean})^2$$

$$= (81 + 196 + 144 + 64 + 400 + 225 + 289)/7$$

$$- (13.571429)^2$$

$$= 199.857143 - 184.183685$$

$$= 15.673458$$

$$sd = +SQRT(15.673458) = 3.958972$$

$$t = (13.571429)/(3.958972/2.645751)$$

$$= 9.069683$$

As before, table  $t_{0.05}$  for 6 d.f. for one tailed test = 1.94.

As calculated  $t >$  table  $t$ , the null hypothesis is rejected and we conclude that the PSS score of the case group subjected to music therapy is significantly lowered.

The encouraging results motivated us to build a music therapy app called “MusiHeal”. The working of this app, developed by the second author, is explained next.

## 6. Music therapy app “MusiHeal”

### 1) About the environment:

(1) The app is built on android studio (a software for building mobile applications) using the flutter framework, which targets both the platform devices—android and iOS, from a single code-base. Flutter uses dart programming language (which is C++ based) and hence this mobile app is built on dart.

(2) Database, testing, and analytics will be implemented (if needed in future) using firebase developed by Google.

## 2) About the app:

(1) The app starts with a beautiful “Splash screen”, followed by an interactive instructions interface, and the user will be directed further only after reading all the instructions.

(2) Now the user will be directed to a filter-based interface which will contain five filter categories.

- Age (0–100 years).
- Musical background (yes {low, medium, high} & no).
- Mental health (normal, anxiety disorders, mood disorders).
- Psychotic disorders (dementia).
- Physical health (normal, physically challenged), and music type (Indian, western; both having classical and modern subtypes)

(3) After selecting the filters, the user will be directed to the “home screen” which contains:

- Real-time refreshing “Did you know?” component.
- An option for going to meditation page.
- Help and support option.
- List of symptoms (pain, fever, nausea/vomiting, depression and anxiety, sleep disturbance, breathing problem) from which the user can choose accordingly.

(4) After choosing the symptom, the user will be directed to the “raga song list screen” which will hold a list of raga songs, going from top-to-bottom, the raga element will increase in the list. Selecting any song from the list will redirect them to a “music player screen”. There will also be an option for a pure raga songs list, only for those users who have good knowledge of music, which will be determined from the initial filters.

(5) Now, the “music player screen” will contain a music player interface having elements such as raga-song name, play/pause, current-time/remaining-time, repeat, speaker/headset, favorites, and a container showing the next upcoming raga song.

(6) The “help and support screen” will contain details about the app and some songs, all the instructions, and our team contact details.

(7) The meditation screen will contain the songs list beneficial for meditation, which will be categorized based on the frequency suitable for the user, which will be determined from the initial filters. Selecting any meditative track will lead again to the “music player screen”.

(8) The “pure raga screen” will contain the pure raga soundtracks, and symptom name followed by a filter that will bifurcate the list into instrumental or vocal. Selecting any raga track will lead again to the “music player screen”.

## 7. Discussion

The study plan of our research consists of three phases:

Phase 1: assessing the impact of music especially Hindustani ragas in reducing stress.

Phase 2: assessing the musical properties of the Hindustani ragas and raga based songs (e.g. Tagore songs), helpful in reducing stress, through statistical musicology.

Phase 3: brain imaging study through EEG signals to explore the emotional changes caused in the brain by Hindustani ragas and raga based songs and how they are actually helping in reducing stress.

See Chakraborty and Katyayan<sup>[16]</sup> for further details on our ongoing research.

The work done in this paper refers to phase 1 of the study. The PSS score of the control group not subjected to music therapy worsened possibly due to examination stress, job insecurity and other factors. On the other hand, the PSS score of the case group subjected to music therapy is significantly lowered. In other words, music therapy intervention is able to combat stress, given that the participants were allocated to the control and case groups using randomized control trial and there was no bias in allocation. We propose to extend our research on Hindustani ragas to combat migraine episodes, in the pain

management in cancer patients, lower the anxiety level in pregnant women, combat stress in type 2 diabetes, control hypertension and assess the impact of these ragas in psychiatric cases.

## 8. Concluding remarks

The paired  $t$  results show that music therapy is able to combat stress. The encouraging results motivated us to build a music therapy app called “MusiHeal”. We do believe this app will be of immense value to society in healthcare. The specific Hindustani ragas, raga based songs and other genres of music and songs therein used in the study profitably have been noted. The corresponding emotional changes they bring in the brain would be studied through EEG signals which is reserved as a rewarding future work.

Remark: what kind of physical stimulus leads to what kind of emotional changes in the brain is a subject matter of psychophysics which is a branch of psychology. The interested reader is referred to the book by Roederer<sup>[17]</sup>.

## Author contributions

Conceptualization, SC; methodology, SC; software, AP and PS; validation, SC and AC; formal analysis, SC and AC; investigation, AC; resources, AC, AP and PS; data curation, AC; writing—original draft preparation, SC, AP, AC and PS; writing—review and editing, SC; visualization, SC; supervision, SC; project administration, SC; funding acquisition, SC.

## Acknowledgments

The authors are thankful to IDEA: Technology Innovation Hub @ Indian Statistical Institute, Kolkata for sponsoring this research. We would also like to thank the Vice Chancellor, Prof. Indranil Manna for encouraging and supporting this research. We thank all the artists Dr. (Mrs.) Purnima Chakraborty, D. Mus. (Banaras Hindu University, Varanasi), Mr. Manish Kumar Sharma (Department of Performing and Fine Arts, Ranchi University), Mr. Mrinal

Pathak, Mr. Harsh Gautam, Ms. Apoorva Chakraborty, Mr. Sandeep Hazra and Ms. Aditi Singh for their valuable contributions in the five music therapy sessions. Special thanks go to Mrs. Sushmita Mukherjee for helping the music therapist in the data collection and to both Mrs. Mukherjee and her husband Mr. Animesh Mukherjee for coordinating the music therapy sessions.

## Ethical declaration

The authors hereby declare that they have no conflict of interest. As the participants were 9th semester students of the institute in our department, formal permission from the dean of students’ affairs was taken to carry out the music intervention followed by a formal consent form filled out and signed by the participants of both the control and case group.

## References

1. Thaut MH. Rhythm, music and the brain: Scientific foundations and clinical applications, 1<sup>st</sup> ed. Oxfordshire: Routledge; 2005.
2. Beran J. Statistics in musicology, 1<sup>st</sup> ed. Boca Raton: Chapman and Hall/CRC Press; 2004.
3. Temperley D. Music and probability. Cambridge: MIT Press; 2007.
4. Tewari S, Chakraborty S. Statistical musicology: Embracing Hindustani ragas. New York: Nova Science Publishers; 2022. doi: 10.52305/LCKT9868.
5. Patel AD. Music, language and the brain, 1<sup>st</sup> ed. Oxford: Oxford University Press; 2008.
6. Singh SB, Chandra S, Chakraborty S. A brief survey on music intervention in western and non-western (Indian) music. Med Crave Online Journal of Biology and Medicine 2018; 3(4): 190–194. doi: 10.15406/mojbm.2018.03.00097.
7. Priyadarshini P, Chakraborty S. Using statistical modeling, rate of change of pitch and inter onset interval to distinguish between restful and restless ragas. Communications in Mathematics and Statistics 2017; 5(2): 199–212. doi: 10.1007/s40304-017-0108-7.
8. Chakraborty S, Mazzola G, Tewari S, Patra M. Computational musicology in Hindustani music. Cham: Springer Cham; 2014. doi:

- 10.1007/978-3-319-11472-9.
9. Aldridge D. An overview of music therapy research. *Complementary Therapies in Medicine* 1994; 2(4): 204–216. doi: 10.1016/0965-2299(94)90021-3.
  10. Aldridge D. The music of the body: Music therapy in medical settings. *Advances* 1993; 9(1): 17–35.
  11. Sarkamo T, Soto D. Music listening after stroke: Beneficial effects and potential neural mechanisms. *Annals of the New York Academy of Sciences* 2012; 1252(1): 266–281. doi: 10.1111/j.1749-6632.2011.06405.
  12. Sairam TV. *Reviving raga therapy*. Delhi: NADA Centre for Music Therapy; 2004.
  13. Rammohan GV. *Music therapy: The present scenario*. In: Raju MVR (editor). *Health psychology and counselling*. New Delhi: Discovery Publishing House; 2009.
  14. Singh SB, Chakraborty S, Jha KM, *et al.* Impact of Hindustani ragas on visual acuity, spatial orientation and cognitive functions in patients with cerebrovascular accident and diffuse head injury. *Music and Medicine* 2013; 5(2): 67–75. doi: 10.47513/mmd.v5i2.212.
  15. Perceived stress scale [Internet]. Concord: NH Department of Administrative Services; [accessed 2022 Nov 1]. Available from: <https://www.das.nh.gov/wellness/Docs%5CPerceived%20Stress%20Scale.pdf>.
  16. Chakraborty S, Katyayan N. Statistical musicology with therapeutic applications. *Med Crave Online Journal of Biology and Medicine* 2023; 8(2): 50–53. doi: 10.15406/mo-jbm.2023.08.00183.
  17. Roederer J. *The physics and psychophysics of music: An introduction*, 4<sup>th</sup> ed. New York: Springer New York; 2008. doi: 10.1007/978-0-387-09474-8.

# Conservation laws, exact solutions and nonlinear dispersion: A lie symmetry approach

Adnan Shamaoon<sup>1,\*</sup>, Zartab Ali<sup>2</sup>, Qaisar Maqbool<sup>3</sup>

<sup>1</sup> Department of Mathematics, Physics and Electrical Engineering, Northumbria University Newcastle, Newcastle upon Tyne NE1 8ST, U.K. E-mail: adnan.shamaoon@northumbria.ac.uk

<sup>2</sup> Department of Mathematics, Lahore University of Management Sciences, Lahore 54792, Pakistan

<sup>3</sup> Department of Physics, University of Okara, Okara 56300, Pakistan

## ARTICLE INFO

Received: 5 May 2023

Accepted: 21 June 2023

Available online: 26 June 2023

<http://dx.doi.org/10.59400/jam.v1i1.95>

Copyright © 2023 Author(s).

Journal of AppliedMath is published by Academic Publishing Pte. Ltd. This article is licensed under the Creative Commons Attribution License (CC BY 4.0). <http://creativecommons.org/licenses/by/4.0/>

**ABSTRACT:** In this study, we investigated a set of equations that exhibit compact solutions and nonlinear dispersion. We used the classical lie symmetry approach to derive ordinary differential equations (ODEs) that are well suited for qualitative study. By examining the dynamic behavior of these ODEs, we gained insights into the intricate nature of the underlying system. We also used a powerful multiplier approach to establish nontrivial conservation laws and exact solutions for these equations. These conservation laws provide essential information regarding the underlying symmetries and invariants of the system, and shed light on its fundamental properties.

**KEYWORDS:** lie symmetries; infinitesimals operator; conservation laws; Euler-Lagrangian operator; nonlinear dispersion; exact solutions; multipliers approach

## 1. Introduction

Nonlinear waves are waves that exhibit non-linear behavior, meaning that their amplitude and velocity are not linearly related. Solitons and compactons are two types of nonlinear waves. Solitons are stable pulse-like waves that can exist in some nonlinear systems. They can pass through each other without being destroyed, and they can retain their shape even after interacting with other waves. Compactons are a special type of soliton that does not have exponential tails. Solitons and compactons are used as building blocks to formulate the complex dynamical behavior of wave systems throughout science. They have been studied in a variety of fields, including hydrodynamics, nonlinear optics, plasmas, shock waves, tornadoes. Solitons have also acquired prominence in the fields of quantum mechanics and nanotechnology, particularly in the study of nano-hydrodynamics. The solitary wave dynamics<sup>[1]</sup> of the local fractional Bogoyavlensky

Konopelchenko model is a topic of active research in the field of nonlinear wave theory. The local fractional Bogoyavlensky Konopelchenko model is a partial differential equation (PDE) that describes the propagation of waves in a nonlinear medium. The model is a generalization of the classical Bogoyavlensky Konopelchenko model, and it takes into account the effects of fractional diffusion. It is well known that while conventional nonlinearity's influence does not significantly alter with spatial dimension, dispersive processes become more effective at disseminating information. As a result, a model that is well-balanced in one dimension becomes unbalanced in higher dimensions. As a result, strong solitonic structures are often far less common in higher spatial dimensions. Rosenau and Hyman<sup>[2]</sup> presented the compactons, solitons with a compact support, almost 20 years ago using the  $C(l, p)$  model equation in its simplest form,

$$A_y + lA^{l-1}A_z + p(A^{p-1}A_z)_{zz} = 0 \quad l, p > 1 \quad (1)$$

and exact solutions as well as symmetry reductions were derived in the work of Bruzón and Gandarias<sup>[3]</sup>, Bruzón et al.<sup>[4]</sup>, and Anco and Bluman<sup>[5]</sup>. Naz<sup>[6]</sup> utilized the multiplier technique to construct the conservation laws for the equation. Because the authors believe that higher order multipliers determining equations are very complicated and cannot be manually separated, only multipliers of the kind  $M(y, z, A)$  were considered in her work of Conservation laws for some compacton equations using the multiplier approach<sup>[6]</sup>.

In their work, Rosenau and Oron<sup>[7]</sup> investigated how several symbolic forms of nonconvex convection affected the development of compact patterns. To do this, a basic model with cubic dispersion and numerous versions on a nonlinear modified dispersion are utilized which is of the form.

$$\begin{aligned} A_y + (A^3 - A^2)_z + [A(A^2)_{zz}]_z &= 0 \\ A_y + (A^3 - A^2)_z + 2(AA_z)_{zz} &= 0 \end{aligned} \tag{2}$$

In contrast to the  $C(n, n)$  compactons, the breadth of the current compactons varies on their velocity. In a recent study<sup>[8]</sup>, Gandarias has successfully identified and formulated several conservation laws that are not simple or obvious. Furthermore, we have demonstrated that certain equations, which have solutions in the form of compactons and exhibit cubic dispersion, possess a unique property called nonlinear self-adjointness. This discovery is significant as it highlights the intricate dynamics and properties of these equations, providing valuable insights into their behavior and characteristics.

Conservation laws are widely recognized as crucial components in solving equations or systems of differential equations. While not all conservation laws in partial differential equations (PDEs) have direct physical interpretations, they serve a significant purpose in studying the integrability of PDEs. Understanding and identifying these conservation laws are vital steps in comprehending the behavior and properties of

PDEs and their solutions.

The Noether theorem<sup>[2]</sup> is a powerful tool for deriving conservation laws in variational problems. It can be used to derive conservation laws for variational problems, which are problems that can be formulated in terms of a Lagrangian. However, for nonvariational situations, alternative methods are needed to construct conservation laws. Anco and Bluman<sup>[9]</sup> introduced an algorithmic technique that allows for the identification of all conservation laws for evolution equations. Ibragimov<sup>[10]</sup> presented a unique approach based on adjoint equations for nonlinear equations, which eliminates the need for function integrals and does not rely on Lagrangians. The concept of strictly self-adjoint equations<sup>[11-13]</sup> has been expanded upon, and Ibragimov's findings have sparked further research on self-adjointness and its relevance to partial differential equations (PDEs)<sup>[14-23]</sup>. This approach represents an extension of the previously described formula in work of direct construction of conservation laws from field equations<sup>[9]</sup>, providing a broader framework for studying and applying conservation laws in PDEs.

In this research, we will solve the Equation (2) using the lie classical technique, as well as the multipliers approach to derive conservation laws for these equations.

## 2. Derivation of exact solutions from classical lie approach

In this part, we conduct a lie symmetry analysis for a specific system denoted in the Equation (2). We focus on exploring a one-parameter lie group consisting of infinitesimal transformations<sup>[24-26]</sup> in the variables  $(y, z, A)$ . The transformations are expressed in a specific form, which we will investigate and analyze further.

$$\begin{aligned} y^* &= y + \varepsilon\phi(y, z, A) + \vartheta(\varepsilon^2) \\ z^* &= z + \varepsilon\psi(y, z, A) + \vartheta(\varepsilon^2) \\ A^* &= A + \varepsilon\eta(y, z, A) + \vartheta(\varepsilon^2) \end{aligned} \tag{3}$$

where  $\varepsilon$  is the group parameter. To ensure that

the transformation preserves the solutions of Equation (2), it is necessary to satisfy certain conditions. This leads to an overdetermined system of linear equations consisting of eleven equations involving the infinitesimals  $\psi(y, z, A)$ ,  $\phi(y, z, A)$ , and  $\eta(y, z, A)$ . The collection of vector fields that satisfy these equations form the associated lie algebra of infinitesimal symmetries. These vector fields are expressed in the following specific form:

$$\mathbf{X} = \psi \frac{\partial}{\partial z} + \phi \frac{\partial}{\partial y} + \eta \frac{\partial}{\partial A} \tag{4}$$

where  $\mathbf{X}$  is infinitesimal operator or generator of the group. After identifying the infinitesimals, the next step is to solving the invariant surface condition yields the symmetry variables. This condition ensures that the transformed equations remain invariant under the lie symmetry transformations.

$$Y = \psi \frac{\partial A}{\partial z} + \phi \frac{\partial A}{\partial y} - \eta = 0 \tag{5}$$

By considering the determining system for the first formula of Equation (2), we find that the infinitesimals can be expressed as  $\psi = \psi(y, z)$ ,  $\phi = \phi(y)$ , and  $\eta = \eta(y, z, A)$ . These functions, namely  $\psi$ ,  $\phi$ , and  $\eta$ , need to satisfy the following system of equations:

$$\begin{aligned} -3A\psi_z + \phi_y A + 2\eta &= 0, \\ -3A\psi_{zz} + 3\eta_{Ax}A + 4\eta_z &= 0, \\ -2A^2\psi_{zzz} - 3A^2\psi_z + 2A\psi_z - \psi_y + 3A_y A^2 + 6\eta_{Azz}A^2, \\ -2\phi_y A + 8\eta_{zz}A + 6\eta A - 2\eta &= 0, \\ -12A\psi_z + 3\eta_{AA}A^2 + 4\phi_y A + 4\eta_A A + 4\eta &= 0, \\ -4A\psi_{zz} + 3\eta_{AAx}A^2 + 8\eta_{Az}A + 3\eta_z &= 0, \\ -3\psi_z + \eta_{AAA}A^2 + 4\eta_{AA}A + A_y + 2\eta_A &= 0. \end{aligned} \tag{6}$$

Upon solving the determining equations for  $\psi$ ,  $\phi$ , and  $\eta$ , we are able to determine the lie point symmetry generators that form a two-dimensional lie algebra. These generators are obtained as a result of the solutions to the determining equations, and they characterize the symmetries admitted by the Equation (2).

$$\begin{aligned} \mathbf{X}_1 &= \frac{\partial}{\partial z} \\ \mathbf{X}_2 &= \frac{\partial}{\partial y} \end{aligned} \tag{7}$$

In this section, we successfully derived the reduction of the first equation of the Equation (2) to ordinary differential equations (ODEs) using the generators  $\gamma\mathbf{X}_1 + \omega\mathbf{X}_2$ . This reduction allows us to simplify the equation and express it in terms of ODEs, which are typically easier to analyze and solve. Additionally, we obtained the similarity variable and similarity solution.

$$\begin{aligned} \theta &= \omega z + \gamma y \\ A &= \rho(\theta) \end{aligned} \tag{8}$$

Substituting Equation (8) into Equation (5), we obtain:

$$\begin{aligned} 2\omega^3\rho^2\rho_{\theta\theta\theta} + 8\omega^3\rho\rho_{\theta}\rho_{\theta\theta} + 2\omega^3(\rho_{\theta})^3 \\ + 3\omega\rho^2\rho_{\theta} - 2\omega\rho\rho_{\theta} - \gamma\rho_{\theta} &= 0 \end{aligned} \tag{9}$$

After performing the integration of the equation with respect to  $\theta$ , we arrive at the following equation, which takes the form:

$$\begin{aligned} 2\omega^3\rho^2\rho_{\theta\theta} + 2\omega^3\rho(\rho_{\theta})^2 + \omega\rho^3 - \omega\rho^2 - \gamma\rho \\ + \kappa_1 &= 0 \end{aligned} \tag{10}$$

This reduced ordinary differential equation (ODE), given by Equation (10), exhibits a group corresponding to the generator  $\mathbf{H} = \partial_{\theta}$ . This group corresponds to a symmetry of the equation, indicating that there is a transformation along the  $\theta$  direction that leaves the equation invariant.

By considering the invariants of the first prolongation and introducing the new variables as given in equations, namely:

$$\begin{aligned} \rho &= Z \\ \rho' &= v(Z) \\ \rho'' &= v(Z) \frac{dv}{dZ} \end{aligned} \tag{11}$$

we can further simplify Equation (10). This reduction allows us to express Equation (10) as a first-order ordinary differential equation (ODE).

$$2\omega^3 Z^2 v v_z + 2\omega^3 Z v^2 + \omega Z^3 - \omega Z^2 - \gamma Z = 0 \tag{12}$$

whose implicit solution is,

$$12\omega^3 Z^2 v^2 + 3\omega Z^4 - 4\omega Z^3 - 6\gamma Z^2 + 12\kappa_1 Z + \kappa_2 = 0 \tag{13}$$

where  $\kappa_1$  and  $\kappa_2$  are arbitrary constants. Following a similar procedure as before, we apply the same methodology to the second equation of the Equation (2). This leads to the derivation of the generators  $\mathbf{X}_1$  and  $\mathbf{X}_2$ , as well as the determination of the similarity variable and similarity solution given by Equation (8). The corresponding reduced ordinary differential equation (ODE) is then obtained as equation, which takes the form:

$$2\omega^3 \rho \rho_{\theta\theta\theta} + 6\omega^3 \rho_{\theta} \rho_{\theta\theta} + 3\omega \rho^2 \rho_{\theta} - 2\omega \rho \rho_{\theta} - \gamma \rho_{\theta} = 0 \tag{14}$$

By integrating Equation (14) once with respect to  $\theta$ , we arrive at equation:

$$\kappa_1 + 2\omega^3 \rho \rho_{\theta\theta} + 2\omega^3 (\rho_{\theta})^2 + \omega \rho^3 - \omega \rho^2 - \gamma \rho = 0 \tag{15}$$

Equation (15) represents the reduced ODE, which admits the symmetry generator  $\mathbf{H} = \partial_{\theta}$ . By considering the invariants of its first prolongation and introducing the variables given by Equation (11), we can further simplify Equation (15) to obtain the first-order ODE.

$$2\omega^3 Z v v_z + 2\omega^3 v^2 + k_1 + \omega Z^3 - \omega Z^2 - \gamma Z = 0 \tag{16}$$

whose implicit solution is,

$$60\omega^3 Z^2 v^2 + 30Z^2 \kappa_1 + 12\omega Z^5 - 15\omega Z^4 - 20\gamma Z^3 + \kappa_2 = 0 \tag{17}$$

### 2.1 Qualitative study of ODEs

Equations (10) and (15), after setting  $\kappa_1 = 0$ , can be written as:

$$\begin{aligned} \rho'' + \frac{(\rho')^2}{\rho} + \frac{\rho}{2\omega^2} - \frac{1}{2\omega^2} - \frac{\gamma}{2\omega^3 \rho} &= 0 \\ \rho'' + \frac{(\rho')^2}{\rho} + \frac{\rho^2}{2\omega^2} - \frac{\rho}{2\omega^2} - \frac{\gamma}{2\omega^3} &= 0 \end{aligned} \tag{18}$$

By introducing the change of variables  $z = \rho$  and  $\varphi = \rho' \rho$ , the Equations (18) can be transformed into a system of the form,

$$\begin{aligned} \dot{z} &= \frac{\varphi}{z} \\ \dot{\varphi} &= \varrho(z) \end{aligned} \tag{19}$$

where,

$$\begin{aligned} \varrho(z) &= -\frac{1}{2\omega^2} z^2 + \frac{1}{2\omega^2} z + \frac{\gamma}{2\omega^3} \\ \varrho(z) &= -\frac{1}{2\omega^2} z^3 + \frac{1}{2\omega^2} z^2 + \frac{\gamma}{2\omega^3} z \end{aligned} \tag{20}$$

respectively.

The phase portrait of the Equation (19) is divided into two half-planes that are invariant, one for  $z > 0$  and the other for  $z < 0$ . This means that the dynamics of the system in each half-plane remains confined within that respective half-plane. Equation (19) is conservative, meaning that there exist conserved quantities associated with it. These conserved quantities are defined by the differentiable functions  $\mathbf{P}$ , given by

$$\begin{aligned} \mathbf{P}(z, \varphi) &= \frac{\varphi^2}{2} + \frac{z^4}{8\omega^2} - \frac{z^3}{6\omega^2} - \frac{\gamma z^2}{4\omega^2} \\ \mathbf{P}(z, \varphi) &= \frac{\varphi^2}{2} + \frac{z^5}{10\omega^2} - \frac{z^4}{8\omega^2} - \frac{\gamma z^3}{6\omega^3} \end{aligned} \tag{21}$$

These quantities remain constant along the trajectories of the system, meaning that  $\frac{d\mathbf{P}}{dt} = \mathbf{P}_z \dot{z} + \mathbf{P}_{\varphi} \dot{\varphi} = 0$ . Therefore, the trajectories lie on curves defined by  $\mathbf{P}(z, \varphi)$  is equal to constant, and they exhibit symmetry relative to the  $z$ -axis. Importantly,  $\mathbf{P}(z, \varphi)$  can be represented as

$$\mathbf{P}(z, \varphi) = \frac{\varphi^2}{2} + \mathfrak{R}(z) \tag{22}$$

where  $\mathfrak{R}(z)$  is given by

$$\mathfrak{R}(z) = -\int_0^z v \varrho(v) dv \tag{23}$$

The equilibrium points  $\mathcal{P}$  of the Equation (19), if they exist, are located on the  $z$ -axis and correspond to the critical points of  $\mathbf{P}(z, \varphi)$ . This

can be seen by analyzing the partial derivatives of  $\mathbf{P}(z, \varphi)$  with respect to  $z$  and  $\varphi$ .

$$\begin{aligned} \frac{\partial \mathbf{P}}{\partial z} &= -z\varrho(z) = 0 \\ &\Leftrightarrow \dot{\varphi} = 0 \\ \frac{\partial \mathbf{P}}{\partial \varphi} &= \varphi = 0 \\ &\Leftrightarrow \dot{z} = 0 \end{aligned} \tag{24}$$

The equilibrium point  $\mathcal{P}(z^*, 0)$  is a fixed point of the Equation (19) if  $z^*$  is a critical point of  $\mathfrak{R}(z)$ , i.e., a zero of the polynomial function  $\varrho(z)$  defined in Equation (21).

### 3. Multipliers approach

In their work, Anco and Bluman<sup>[5]</sup> presented a general method for deriving conservation laws for partial differential equations in a Cauchy-Kovaleskaya form, specifically for evolution equations of the form,

$$A_y = E(z, A, A_z, A_{zz}, \dots, A_{nz}) \tag{25}$$

The conservation laws are characterized by a multiplier  $\Lambda$  that does not depend on  $A_y$  and satisfies the following equation

$$F[A] \left( \Lambda A_y - \Lambda G(z, A, A_z, A_{zz}, \dots, A_{nz}) \right) = 0 \tag{26}$$

where, the Euler-Lagrangian operator  $F[A]$  is defined as

$$F[A] = \frac{\partial}{\partial A} - D_y \frac{\partial}{\partial A_y} - D_z \frac{\partial}{\partial A_z} + D_z^2 \frac{\partial}{\partial A_{zz}} + \dots \tag{27}$$

where,  $D_y$  and  $D_z$  are the total derivatives with respect to  $y$  and  $z$ . The conserved vector is required to satisfy

$$\Lambda = F[A]Y^y \tag{28}$$

and the flux  $Y^z$  is given by Euler<sup>[27]</sup>.

$$Y^z = -D_z^{-1}(\Lambda E) - \frac{\partial Y^y}{\partial A_z} E + E D_z \left( \frac{\partial Y^y}{\partial A_{zz}} \right) + \dots \tag{29}$$

The conservation law will be written as

$$D_y(Y^y) + D_z(Y^z) = 0 \tag{30}$$

We get the following multipliers: for first equation of Equation (2).

$$\begin{aligned} \Lambda &= 1 \\ \Lambda &= A \\ \Lambda &= A^2 A_{zz} + \frac{A^3}{2} - \frac{A^2}{2} + A A_z^2 \end{aligned} \tag{31}$$

For second equation of the Equation (2),

$$\begin{aligned} \Lambda &= 1 \\ \Lambda &= A^2 \end{aligned} \tag{32}$$

we have the equation, which represents the first equation of the Equation (2).

$$G \equiv A_y + (A^3 - A^2)_z + [A(A^2)_{zz}]_z = 0 \tag{33}$$

Equation (33) can be considered nonlinearly self-adjoint if there exists a nontrivial function  $\rho(y, z, A, A_z, \dots)$ , such that when we substitute  $v = \rho(y, z, A, A_z, \dots)$  into the adjoint equation such that  $\rho(y, z, A, A_z, \dots) \neq 0$ , it becomes same as the original Equation (33); that is

$$G_{|v=\rho}^* = \gamma G \tag{34}$$

To do so, we consider its adjoint equation to Equation (33) is following, where  $v$  is a new dependent variable,

$$G^* \equiv \frac{\delta(vG)}{\delta A} = 0 \tag{35}$$

where,

$$\frac{\delta}{\delta A} = \frac{\partial}{\partial A} - D_y \left( \frac{\partial}{\partial A_y} \right) - D_z \left( \frac{\partial}{\partial A_z} \right) + D_z^2 \left( \frac{\partial}{\partial A_{zz}} \right) \tag{36}$$

Equation (36) defines the variational derivative, also known as the Euler-Lagrangian operator. The variational derivative takes into account the total differentiations with respect to  $y$  and  $z$ , denoted by  $D_y$  and  $D_z$ , respectively.

Let us select nonlinearly self-adjoint equations from

$$\begin{aligned}
 G^* - \gamma(A_y + (A^3 - A^2)_z + [A(A^2)_{zz}]_z) & \quad \rho = 1 \\
 - \omega(A_y + (A^3 - A^2)_z & \quad \rho = A^2 \\
 + [A(A^2)_{zz}]_z) & \\
 - \epsilon(A_y + (A^3 - A^2)_z & \\
 + [A(A^2)_{zz}]_z)_{zz} = 0 & \quad (42)
 \end{aligned}$$

where  $\gamma, \omega,$  and  $\epsilon$  are undetermined coefficients. Setting  $v = \rho(y, z, A, A_z, A_{zz})$ , we can analyze the coefficients for the different derivatives of  $A$  in order to determine the requirements for the equation to be nonlinearly self-adjoint. We conclude that the following requirements must be met

$$\begin{aligned}
 \gamma &= -\rho_A \\
 \omega &= -\rho_{A_z} \\
 \epsilon &= -\rho_{A_{zz}}
 \end{aligned} \quad (38)$$

and by resolving the remaining equations, we obtain

$$\rho = \kappa_1 A^2 A_{zzz} + \kappa_1 A A_z^2 + c(A) A_z + d(A) \quad (39)$$

with

$$\begin{aligned}
 c(A) &= \kappa_2 A^{\frac{4}{3}} \\
 d(A) &= \frac{1}{2} (\kappa_1 A^3 - \kappa_1 A^2) + \kappa_3 A + \kappa_4
 \end{aligned} \quad (40)$$

The following are the outcome.

- In the given Equation (2), the first equation is stated to be nonlinearly self-adjoint.

$$\begin{aligned}
 \rho &= 1 \\
 \rho &= A \\
 \rho &= A^2 A_{zz} + \frac{A^3}{2} - \frac{A^2}{2} + A A_z^2
 \end{aligned} \quad (41)$$

Using the same method on the second equation of Equation (2), we get the following conclusion.

- For the second equation of the Equation (2) to be nonlinearly self-adjoint, we are given the following choices for the function  $\rho(y, z, A, A_z, A_{zz})$ ,

The functions  $\rho(y, z, A, A_z, A_{zz})$  derived from the condition of nonlinear self-adjointness in the equations correspond to the multipliers used in the Anco and Bluman method<sup>[5]</sup> for the direct construction of conservation laws.

## 4. Conservation laws

We obtain the conserved quantities (vectors) and fluxes associated with the multipliers from Equations (28) and (29). For the first equation of Equation (2):

### 4.1 First conserved vector

$$\begin{aligned}
 \Lambda &= 1 \\
 \eta^y &= A \\
 \eta^z &= A(A^2 + (-1 + 2A_{zz})A + 2A_z^2)
 \end{aligned} \quad (43)$$

### 4.2 Second conserved vector

$$\begin{aligned}
 \Lambda &= A \\
 \eta^y &= \frac{A^2}{2} \\
 \eta^z &= \frac{3}{4} A^4 - \frac{2}{3} A^3 + 2A^3 A_{zz} + A^2 A_z^2
 \end{aligned} \quad (44)$$

### 4.3 Third conserved vector

$$\begin{aligned}
 \Lambda &= A^2 A_{zz} + \frac{A^3}{2} - \frac{A^2}{2} + A A_z^2 \\
 \eta^y &= -\frac{1}{2} A^2 + \frac{1}{8} A^4 - \frac{1}{6} A^3 \\
 \eta^z &= \frac{1}{4} (A^4 + (4A_{zz} - 2)A^3 + \left( 4A_z^2 \right. \\
 & \quad \left. + 4 \left( A_{zz} - \frac{1}{2} \right)^2 A^2 \right) \\
 & \quad + \frac{1}{4} \left( 8 \left( A_{zz} - \frac{1}{2} \right) A_z^2 A + 4A_z^4 \right. \\
 & \quad \left. + 4A_y A_z \right) A^2
 \end{aligned} \quad (45)$$

The following multipliers, conserved densi-

ties and fluxes are obtained for the second equation of Equation (2):

#### 4.4 First conserved vector

$$\begin{aligned}\Lambda &= 1 \\ \eta^y &= A \\ \eta^z &= 2AA_{zz} + 2(A_z)^2 - A^3 + A^2\end{aligned}\quad (46)$$

#### 4.5 Second conserved vector

$$\begin{aligned}\Lambda &= A^2 \\ \eta^y &= \frac{A^3}{3} \\ \eta^z &= \frac{1}{10}A^3(20A_{zz} + 6A^2 - 5A)\end{aligned}\quad (47)$$

Applying the theorem on conservation laws derived from the generators  $\mathbf{X}_1$  and  $\mathbf{X}_2$  in the work of Ibragimov<sup>[10]</sup> may lead to trivial conservation laws in this case. Trivial conservation laws are those that do not provide new information about the system and are often associated with symmetries that are not physically relevant. However, it is worth noting that in the Conservation laws of scaling-invariant field equations<sup>[28]</sup>, a method is presented specifically for deriving conservation laws associated with scaling symmetries. This method may provide more meaningful conservation laws for the system. If scaling symmetries are present in the system described by Equation (2), applying the method described by Anco<sup>[28]</sup> could yield non-trivial conservation laws.

## 5. Conclusions

We used the classical lie approach to solve two partial differential equations (PDEs) with nonlinear dispersion and compacton solutions. Because these equations have symmetries, we were able to reduce them further into first-order ordinary differential equations (ODEs). This reduction gave useful insights into their dynamic behaviour and qualified them for qualitative

analysis. We used infinitesimal operator of the group and Euler-lagrangian operator to get system of determining equations. The multipliers approach helps us to find exact solutions of our system of differential equations. We also investigated that Equation (2) is nonlinear selfadjointness. When studying the translation generators, we discovered that the conservation laws generated using the conservation laws theorem<sup>[10]</sup>, which removes the necessity for integrating functions, result in some conservation laws that do not give additional information (trivial conservation laws). Using the multipliers technique, we were able to generate nontrivial conservation laws using integral formulae, which improved our knowledge of the system's conservation properties.

## Author contributions

Conceptualization, AS and ZA; methodology, AS; software, QM; formal analysis, ZA; investigation, AS; resources, ZA; data curation, AS; writing—original draft preparation, AS and QM; writing—review and editing, AS and QM; visualization, AS; supervision, AS; funding acquisition, ZA and QM. All authors have read and agreed to the published version of the manuscript.

## Conflict of interest

The authors declare no conflict of interest.

## References

1. Wang K. Solitary wave dynamics of the local fractional Bogoyavlensky-Konopelchenko model. *Fractals* 2023; 31(5): 2350054. doi: 10.1142/S0218348X23500548
2. Rosenau P, Hyman JM. Compactons: Solitons with finite wavelength. *Physical Review Letters* 1993; 70(5): 564–567. doi: 10.1103/PhysRevLett.70.564
3. Bruzón MS, Gandarias ML. Traveling wave solutions of the  $K(m, n)$  equation with generalized evolution. *Mathematical Methods in the Applied Sciences* 2018; 41(15): 5851–5857. doi: 10.1002/mma.1339

4. Bruzón MS, Gandarias ML, González GA, Hansen R. The  $K(m, n)$  equation with generalized evolution term studied by symmetry reductions and qualitative analysis. *Applied Mathematics and Computation* 2012; 218(20): 10094–10105. doi: 10.1016/j.amc.2012.03.084
5. Anco SC, Bluman G. Direct construction method for conservation laws of partial differential equations part II: General treatment. *European Journal of Applied Mathematics* 2002; 13(5): 567–585. doi: 10.1017/S0956792501004661
6. Naz R. Conservation laws for some compacton equations using the multiplier approach. *Applied Mathematics Letters* 2012; 25(3): 257–261. doi: 10.1016/j.aml.2011.08.019
7. Rosenau P, Oron A. On compactons induced by a non-convex convection. *Communications in Nonlinear Science and Numerical Simulation* 2014; 19(5): 1329–1337. doi: 10.1016/j.cnsns.2013.09.028
8. Gandarias ML. Conservation laws for some equations that admit compacton solutions induced by a non-convex convection. *Journal of Mathematical Analysis and Applications* 2015; 430(2): 695–702. doi: 10.1016/j.jmaa.2015.04.071
9. Anco SC, Bluman G. Direct construction of conservation laws from field equations. *Physical Review Letters* 1997; 78(15): 2869–2873. doi: 10.1103/PhysRevLett.78.2869
10. Ibragimov NH. A new conservation theorem. *Journal of Mathematical Analysis and Applications* 2007; 333(1): 311–328. doi: 10.1016/j.jmaa.2006.10.078
11. Ibragimov NH. Quasi-self-adjoint differential equations. *Archives of ALGA* 2007; 4: 55–60.
12. Gandarias ML. Weak self-adjoint differential equations. *Journal of Physics A: Mathematical and Theoretical* 2011; 44(26): 262001. doi: 10.1088/1751-8113/44/26/262001
13. Ibragimov NH. Nonlinear self-adjointness and conservation laws. *Journal of Physics A: Mathematical and Theoretical* 2011; 44: 432002. doi: 10.1088/1751-8113/44/43/432002
14. Bruzón MS, Gandarias ML, Ibragimov NH. Self-adjoint sub-classes of generalized thin film equations. *Journal of Mathematical Analysis and Applications* 2009; 357(1): 307–313. doi: 10.1016/j.jmaa.2009.04.028
15. Gandarias ML, Bruzón MS. Some conservation laws for a forced KDV equation. *Nonlinear Analysis: Real World Applications* 2012; 13(6): 2692–2700. doi: 10.1016/j.nonrwa.2012.03.013
16. Freire IL. Self-adjoint sub-classes of third and fourth-order evolution equations. *Applied Mathematics and Computation* 2011; 217(22): 9467–9473. doi: 10.1016/j.amc.2011.04.041
17. Freire IL, Sampaio JCS. On the nonlinear self-adjointness and local conservation laws for a class of evolution equations unifying many models. *Communications in Nonlinear Science and Numerical Simulation* 2014; 19(2): 350–360. doi: 10.1016/j.cnsns.2013.06.010
18. Ibragimov N, Torrisi M, Tracinà R. Quasi self-adjoint nonlinear wave equations. *Journal of Physics A: Mathematical and Theoretical* 2010; 43(44): 442001. doi: 10.1088/1751-8113/43/44/442001
19. Ibragimov NH, Torrisi M, Tracina R. Self-adjointness and conservation laws of a generalized burgers equation. *Journal of Physics A: Mathematical and Theoretical* 2011; 44: 145201. doi: 10.1088/1751-8113/44/14/145201
20. Gandarias ML. Weak self-adjointness and conservation laws for a porous medium equation. *Communications in Nonlinear Science and Numerical Simulation* 2012; 17(6): 2342–2349. doi: 10.1016/j.cnsns.2011.10.020
21. Gandarias ML, Redondo M, Bruzón MS. Some weak self-adjoint Hamilton—Jacobi—Bellman equations arising in financial mathematics. *Nonlinear Analysis: Real World Applications* 2012; 13(1): 340–347. doi: 10.1016/j.nonrwa.2011.07.041
22. Gandarias ML. Nonlinear self-adjointness through differential substitutions. *Communications in Nonlinear Science and Numerical Simulation* 2014; 19(10): 3523–3528. doi: 10.1016/j.cnsns.2014.02.013
23. Torrisi M, Tracinà R. Quasi self-adjointness of a class of third order nonlinear dispersive equations. *Nonlinear Analysis: Real World Applications* 2013; 14(3): 1496–1502. doi: 10.1016/j.nonrwa.2012.10.013
24. Deiakeh RA, Arqub OA, Smadi MA, Momani S. Lie symmetry analysis, explicit solutions, and conservation laws of the time-fractional Fisher equation in two-dimensional space. *Journal of Ocean Engineering and Science* 2022; 7(4): 345–352. doi: 10.1016/j.joes.2021.09.005
25. Arqub OA, Hayat T, Alhodaly M. Analysis of lie symmetry, explicit series solutions, and conservation laws for the nonlinear time-fractional

- phi-four equation in two-dimensional space. *International Journal of Applied and Computational Mathematics* 2022; 8(3): 145. doi: 10.1007/s40819-022-01334-0
26. Aal MA, Arqub OA. Lie analysis and laws of conservation for the two-dimensional model of Newell—Whitehead—Segel regarding the Riemann operator fractional scheme in a time-independent variable. *Arab Journal of Basic and Applied Sciences* 2023; 30(1): 55–67. doi: 10.1080/25765299.2023.2172840
27. Euler N, Euler M. On nonlocal symmetries, nonlocal conservation laws and nonlocal transformations of evolution equations: Two linearisable hierarchies. *Journal of Nonlinear Mathematical Physics* 2009; 16(4): 489–504. doi: 10.1142/S1402925109000509
28. Anco SA. Conservation laws of scaling-invariant field equations. *Journal of Physics A: Mathematical and General* 2003; 36: 8623. doi: 10.1088/0305-4470/36/32/305



## Academic Publishing Pte. Ltd.

---

Add: 73 Upper PayaLebar Road, #07-02B-06, Centro Bianco, Singapore 534818

Tel: +65 83184869

E-mail: [editorial\\_office@acad-pub.com](mailto:editorial_office@acad-pub.com)

Web: <http://ojs.acad-pub.com/>